1

OCD Work Unit No. 1111G
USNRDL-TR-1045
19 July 1966

AD 645552

EXPERIMENTAL AND CALCULATED ESTIMATES OF THE SHIELDING EFFECTIVENESS OF COMPARTMENTED STRUCTURES EXPOSED TO FALLOUT

by

B.W. Shumway

U.S. NAVAL RADIOLOGICAL DEFENSE LABORATORY

SAN FRANCISCO · CALIFORNIA · 94135

RADIATION TRANSPORT BRANCH
Dr. A. Goodwin, Head

RADIATION PHYSICS DIVISION
Dr. C. S. Cook, Head

ADMINISTRATIVE INFORMATION

This report was sponsored and funded by the Office of Civil Defense, OCD-PS-64-92, Work Unit 1111G.

DDC AVAILABILITY NOTICE

Distribution of this document is unlimited.

ACCESSION for	
CFSTI	WHITE SECTION ☑
DDC	BUFF SECTION ☐
UNANNOUNCED	
JUSTIFICATION	per statement on Doc
BY	Fm
DISTRIBUTION/AVAILABILITY CODES	
DIST.	AVAIL. and/or SPECIAL
/	

OCD REVIEW NOTICE

This report has been reviewed in the Office of Civil Defense and approved for publication. Approval does not signify that the contents necessarily reflect the views and policies of the Office of Civil Defense.

Eugene P. Cooper

Eugene P. Cooper
Technical Director

D.C. Campbell, CAPT USN
Commanding Officer and Director

ABSTRACT

Exposure reduction factors were measured inside six compartmented steel structures having different wall thicknesses ranging from 1/4 to 1-1/2 in. These were exposed to radiation from fallout of varying age from three to nine days. Calculations based upon the Nelms-Cooper gamma-ray spectrum at H + 1.12 hours were made for selected compartments in each of the structures following procedures given in the Office of Civil Defense Professional Manual, PM-100-1. Comparison of experiment and calculation reveals a sensitivity to spectral changes and shows that protection is greater during the periods D + 3 to D + 9 days than at H + 1.12 hours. Overall agreement is generally satisfactory. The calculational methods for radiation through floors, however, appear to be inadequate.

Spectra measured on site at D + 3 and D + 9 days are given.

SUMMARY

Six cube-shaped steel structures of different wall thicknesses were exposed to fallout radiation at the Nevada Test Site at various times from D + 3 to D + 9 days. Each structure contained 27 compartments in which ionization chambers were placed. The exterior and interior walls of each structure were of the same thickness. The free-field exposure rate at 3-ft height was measured continuously so that protection provided by the structures could be estimated generally within an accuracy of 5 percent. Corrections for ground roughness were made.

Experimentally determined, time-integrated reduction factors were compared with calculated values using the OCD Professional Manual, PM-100-1. The calculated reduction factors were always smaller by amounts ranging from 14 to 100 percent, a not surprising result since the calculational methods were based upon the more energetic gamma rays emitted by 1.12-hour fission products. The thicker-walled structures showed greater differences between calculated and experimental reduction factors. Most, but probably not all, of the differences may be ascribed to changes in the gamma-ray spectrum. Spectra were measured on site at D + 3 and D + 9 days. These when compared with the H + 1.12 hour spectrum could be correlated with the experimental reduction factors but not conclusively.

Contributions through various walls are shown graphically and indicate that most of the refinements of the OCD PM-100-1 methods were not tested sensitively. Because of the exponential character of attenuation, radiation through the thinner pathways of the structures tended to mask other shielding effects. Since the bottom surfaces of the structures, which were placed 4 ft above the ground, were shielded with 2 in. of lead, differences were detected between exposures on the bottom story and the middle story. These differences when compared with calculations suggest that the present method for treating radiation through floors underestimates the radiation that reaches a detector after passing through the walls of the story below.

CONTENTS

LIST OF TABLES

LIST OF FIGURES

SUMMARY OF REPORT

EXPERIMENTAL AND CALCULATED ESTIMATES OF THE SHIELDING EFFECTIVENESS OF COMPARTMENTED STRUCTURES EXPOSED TO FALLOUT

USNRDL-TR-1045, dated 19 July 1966

by B. W. Shumway

Time-integrated exposures were measured within compartmented structures in a fallout field at the Nevada Test Site at various times from D+3 to D+9 days. The measurements provide experimental reduction factors which can be compared with shielding calculations.

In order to insure the usefulness of the measurements the external radiation field was studied in detail. The free-field exposure rate 3 ft above the earth's surface was measured continuously. The gamma-ray spectrum was measured both azimuthally and at various angles of elevation through 180 degrees. The effective roughness of the surface in attenuating radiation was evaluated by two methods, and the contamination density of a square area 600 ft on a side was sampled both as photon irradiation and 4π exposure rate at 3 ft.

In all, six cubic steel structures 30 in. on a side were used. Each contained 27 compartments instrumented with ionization chambers. The walls both internal and exterior were of uniform thickness for a given structure. Wall thicknesses of the six structures were 1/4", 3/8", 1/2", 3/4", 1", and 1 1/2".

Calculations of reduction factors were made for selected compartments within each structure using the methods and graphs given in PM-100-1. A ground-roughness correction with τ = 24 ft of air was applied. The calculated reduction factors were then compared with those obtained experimentally and were found to be always smaller by amounts ranging from 14 to 100 percent, a not surprising result since the calculational methods were based upon the more energetic gamma rays emitted by 1.12-hour fission products. The thicker-walled structures showed greater differences between calculated and experimental reduction factors. Most, but probably not all, of the differences may be ascribed to changes in the gamma-ray spectrum. Spectra were measured on site at D+3 and D+9 days. These when compared with the H + 1.12 hour spectrum could be correlated with the experimental reduction factors but not conclusively.

Contributions through various walls are shown graphically and indicate that most of the refinements of the OCD PM-100-1 methods were not tested sensitively. Because of the exponential character of attenuation, radiation through the thinner pathways of the structures

tended to mask other shielding effects. Since the bottom surfaces of the structures, which were placed 4 ft above the ground, were shielded with 2 in. of lead, differences were detected between exposures on the bottom story and the middle story. These differences when compared with calculations suggest that the present method for treating radiation through floors underestimates the radiation that reaches a detector after passing through the walls of the story below.

The accuracy of the experimental results is estimated to be 5 percent. Though spectral differences preclude a satisfactory test of the PM-100-1 methods, these data are relatively unique in that the fallout field was not only real but was also carefully documented. They should prove useful for testing other calculational methods, or for testing PM-100-1 methods provided curves are generated which represent the actual spectra encountered in the field.

INTRODUCTION

During the summer of 1962 a series of compartmented structures was exposed to fallout radiation at the Nevada Test Site. Exposure measurements were made within the various compartments and also at a height of 3 ft in a free-field region near the structures. From these measurements time-integrated reduction factors were calculated as indicators of the structures' shielding effectiveness.[1] These factors were functions of the wall thickness, the position within the structure, and the exposure period.

At the same time supplementary information was obtained regarding the uniformity of the fallout field, the effect of ground roughness upon the exposure as a function of height above the ground, the gamma-ray spectra at various angles, and the change in exposure rate produced by the radioactive decay.

The present report compares the experimental field-test reduction factors with those calculated by use of procedures presented in the Office of Civil Defense Professional Manual, PM-100-1.[2]

THE RADIATION FIELD

Shot Small Boy was the detonation of a low-yield device slightly above the ground surface. Subsequent to the detonation the compartments were placed in the fallout field 9800 ft from Ground Zero and 1300 ft from the most intense radioactive contour (the hot line). Over a square area measuring 600 ft on a side the radiation was sampled at 7 x 7 = 49 stations spaced 100 ft apart. The structures were located approximately at the center of this area.

Contamination densities (as indicated by photon number flux, photons cm^{-2} sec^{-1}) were measured with a collimated NaI(Tl) crystal spectrometer. Along the boundary parallel to and near the hot line the average contamination density was 30 percent higher than the average along the opposite boundary 600 ft away. The average density along the array edge farthest from Ground Zero was about 5-1/2 percent higher than along the edge nearer Ground Zero. The above measurements sampled a geometrical area of 30 sq ft, but the effective area was about 10 sq ft at each station (when weighted by collimator angular response). Measurements with an uncollimated detector would sample much larger areas and consequently might be expected to show less variation. Similar measurements to those mentioned above but with a Victoreen Model 440 survey meter* indicated an average difference of 16 percent in the direction transverse to the hot line and 1 percent along the direction through Ground Zero. A typical exposure rate on the sixth day after detonation was 80 mR/hr.

Gamma-ray energy and angular distributions (photons cm^{-2} MeV^{-1} $steradian^{-1}$) were measured at the beginning of and near the end of the experiments, i.e., on the third and ninth days after the detonation. Over this period the mean energy of the direct radiation as calculated from the fission-product spectrum was expected to be nearly constant, 0.49 to 0.52 MeV, with the value of 0.52 MeV occurring on the ninth day.[3] The mean energy of the D + 9 days spectrum calculated from experimental data was 0.58 MeV.[4] Even though the experimental spectrum included some scattered radiation generally having energies less than 0.2 MeV, the mean energy was yet significantly higher than that given in reference 3.

A comparison of the relative intensities of the source radiation at 1.12 hours, 3 days, and 9 days is shown in Fig. 1. The 1.12-hour relative intensities were calculated from the Nelms-Cooper gamma-ray spectrum[5] thus

$$I_R = E\,S(E)\,\Delta E / \Sigma\, E\,S(E)\,\Delta E$$

where S(E) is the point isotropic source spectrum in photons MeV^{-1} sec^{-1}.**

* Victoreen Instrument Co., 5806 Hough Ave., Cleveland, Ohio 44103.

** E is used in this report in three ways. Here it represents energy. Later it designates a detector location, and finally in Appendix B it represents the eccentricity factor of the PM-100-1 methods.

Since the 3- and 9-day measurements were made at a height of 4 ft above an actual fallout field and accepted photons within a range of angles, the source components as given by the angular flux measurements are not precisely equivalent to S(E). The relative intensities are given by

$$I_R \approx E\, N(4', E, \theta)\, \Delta E / \Sigma\, E\, N(4', E, \theta)\, \Delta E$$

where θ is measured from the downward normal to the surface. Variation of I_R with θ will result from selective filtering of the energy components of the spectrum by the atmosphere and ground roughness. Modification of the spectrum at $\theta = 0$ degrees (9-day spectrum) is considered negligible. Examination of the same spectrum at 70 degrees showed that definite modification had taken place but that it was small. We conclude that the 3-day spectrum favors higher energy photons slightly, but nevertheless is a good approximation to the source radiation. Reference 4 gives additional spectra at various azimuthal and elevation angles.

THE COMPARTMENTED STRUCTURES

Six steel structures, each containing 27 compartments in a cubic 3 x 3 x 3 arrangement, were exposed. Each of the structures had a different wall thickness. For a given structure both interior and exterior walls had the same nominal thickness throughout. The six thicknesses were 1/4, 3/8, 1/2, 3/4, 1, and 1-1/2 in. The outside measurements of the structures were approximately 30 in. on each side. Pedestals, 41 in. high, supported the compartments. The top of each pedestal had a 2 in. thickness of lead which served to shield the structure from radiation coming from directly below. By placing the structures on pedestals, we reduced the effects of minor terrain variations upon the angular distribution of the incident radiation.

The influence of surface roughness upon the radiation field was evaluated by two methods. From dose-vs.-height measurements the roughness was estimated to be equivalent to an overlayer of 22 ft of air, but from angular spectra data it was estimated to be equivalent to 24 ft.[4] In the calculation of protection factors the roughness was assumed to be represented by 24 ft of air.

INSTRUMENTATION

Exposure measurements were made with Baldwin-Farmer Type BD-11 ionization chambers* placed at the center of each compartment. These have a nominal sensitivity of 580 volts per roentgen and are normally charged to 300 volts or less. In order to extend the range of the chambers to 2 R, we applied 1135 volts by means of the special charging-reading circuit shown in Fig. 2. After the radiation-induced change in charge was shared with a 57 pf. capacitor, the resulting voltage was read with a Cary Model 31 vibrating reed electrometer.** Total discharge of the chamber gave a reading of 26.5 volts. The electrometer contains a shorting switch which when closed applies the full charging voltage to the ionization chamber.

Additional dosimetry with photographic film was executed by placing film packages on both surfaces of each wall, floor, and ceiling. When calibrated with Co^{60} gamma rays to give equivalent roentgens, the films gave readings that were about 60 percent of those obtained with ionization chambers. When later extensive calibrations of the film package were made we found strong energy and angular dependence which places doubt upon the film results. The chamber data are considered valid and have been used for the reduction factors in this report.

In order to obtain reduction factors as measures of the shielding effectiveness of the structures, recordings of free field exposure rate were made 3 ft above the ground. The instrument used for this purpose was an ionization chamber with a recycling electronic circuit which recorded a pulse for each 0.243 mR exposure increment along with equally spaced timing pulses. This instrument (GITR) has been used extensively for nuclear-weapon tests.[6] From the continuous recordings, integrated free exposure rates were summed over the appropriate exposure times for the compartmented structures.

The sums, designated as $\overset{\gamma}{D}_{0}$, were corrected for ground roughness (equivalent to 24 ft of air) by using Fig. 28a of NBS Monograph 42,[7] which gives the ratio of exposure rate at various heights to the exposure rate at 3 ft above a smooth plane of infinite extent contaminated with 1.12-hr fission products. Specifically, the correction was

$$L(3' + 24') = 0.61.$$

* Baldwin Instrument Co., Ltd., Dartford, Kent, U.K.
** Applied Physics Corp., 2724 S. Peck Rd., Monrovia, Calif. 91016.

By dividing the experimental exposures $\tilde{D}_G$ by this factor, we obtain the exposure $\tilde{D}_o$ expected over a smooth plane with the same contamination density as was present during the experiments.

Though changes in the gamma-ray spectrum with time may modify the value of L, we assume here that it remains constant. In reference 7, Figs. 28.2a, B-11, and B-12 give values of L for 1.12-hr fission products, Co^{60}, and Cs137 respectively. For a height of 27 ft these curves indicate that the ratio L varies only about 2 percent. If lower energies were abundantly present, a greater variation in L might be expected; but nevertheless should be small.

Table 1 gives the time-integrated free-field exposures for each structure. Both the measured and roughness-corrected values are given.

RESULTS

Values of D_o were divided into the exposures measured within the compartments to give reduction factors, i.e.,

$$\tilde{R} = \int_{t_1}^{t_2} D(X,p,d,t)dt / \int_{t_1}^{t_2} D_o(3',t)$$

$$= \tilde{D}(X,p,d,t_i \rightarrow t_f) / \tilde{D}_o(3',t_i \rightarrow t_f).$$

Here X = effective mass thickness, lbs/ft^2 concrete
p = position of detector within the structure
d = effective height of detector above contaminated surface = h + τ
t = time after detonation

Before discussing the compartment designations some thought should be given to $\tilde{R}$. One would expect that for this ratio to be valid the detectors should be free from energy dependence, since in general the radiation inside the compartment will be harder than in the free field.

Table 1

FREE-FIELD EXPOSURE

Nominal Wall Thickness of Structure (in.)	Exposure Period H + hours from t_1	to t_f	Time-Integrated Free-Field Exposure at 3-ft Height (roentgens) Measured[a] $\tilde{D}_G$	$\tilde{D}_o$ [b]
1/4	95.5	119.2	4.48	7.34
3/8	74.5	91.9	4.43	7.26
1/2	122.7	165.6	5.86	9.62
3/4	74.5	119.2	9.71	15.9
1	167.5	261.9	8.76	14.4
1-1/2	74.5	165.6	16.14	26.5

a. $\tilde{D}_G \equiv \int_{t_1}^{t_2} D(3' + \tau)dt \equiv \tilde{D}(3' + \tau,\ t_1 \rightarrow t_2)$

b. $\tilde{D}_o = \tilde{D}_G / L = D(3',\ t_1 \rightarrow t_2)$

Where: $L = D(3' + \tau,\ 1.12\ \text{hr})/D(3',\ 1.12\ \text{hr}) = 0.61$ is given in reference 7, Fig. 28.2a

τ = ground roughness equivalent thickness, 24 ft of air

We are, however, concerned primarily with protecting people, consequently the free-field measurements should include only the radiation components which are significantly hazardous. If the exposure at the center of the human body is considered the critical factor, then we should establish a low-energy cutoff for the detector so that the free-field dose would become smaller. Alpen[8] has suggested that for acute mortality photon radiation becomes less effective below 80 keV. At 30 keV two times as much exposure is required, and at 15 keV about 100 times as much, to produce equal effect. The spectra given in reference 4 indicate that the free-field exposure from radiation below 100 keV energy relative to the total exposure is small; consequently the low-energy response of the free-field detector was not critical. The GITR, which was used for our measurements, had an abrupt low-energy cutoff just below 70 keV.

Compartment designations are illustrated in Fig. 3, and the measured reduction factors for the compartments are given in Table 2. Since the fallout field was reasonably uniform, reduction factors for compartments in symmetrical positions were grouped and averaged. The data of Table 2 show that the grouping is justified on the basis that the ionization chamber measurements were remarkably reproducible, despite the extended periods of exposure under adverse conditions. The errors shown are standard deviations of individual measurements and include variation resulting from nonuniformity of the fallout field as well as instrument reproducibility. Since there were four values averaged for these compartments, the standard errors of the means will be one-half the indicated errors. The standard deviations do not include systematic errors such as the effects of atmospheric temperature and pressure variations during the exposure periods. On the basis of both calculations and additional experiments the systematic errors are believed to be less than 5 percent.[1]

Those data which do not show error estimates represent single readings, but their accuracy should be comparable to that of the other readings.

STRUCTURE ANALYSIS

Though various calculational procedures might be used to compare with the experimental reduction factors, two sorts of methods are of particular interest, the barrier-geometry factor methods (PM-100-1) of

Table 2

$\tilde{R}$, EXPOSURE REDUCTION FACTORS D/D_o

Compartment Designation		Nominal Wall Thickness (in.)					
		1/4	3/8	1/2	3/4	1	1-1/2
Third Story	A	.253±.003	.204±.003	.160±.003	.110±.006	.093±.004	.0445±.0007
	B	.221±.003	.168±.003	.123±.005	.078±.001	.064±.006	.0270±.0007
	C	.189	.122	.084	-	.036	.0074
Second Story	D	.250±.009	.198±.003	.157±.003	.108±.002	.092±.004	.048±.006
	E	.216±.003	.162±.003	.124±.003	.076±.001	.062±.003	.0272±.0009
	F	$.18_3$	$.12_1$	.080	$.038_4$	$.029_2$	.0081
First Story	G	.220±.012	.177±.006	.139±.003	.099±.003	.086±.009	.044±.002
	H	.181±.003	.143±.014	.103±.002	.068±.004	.065±.006	.0272±.0015
	I	$.14_0$	.105	.063	$.032_9$	$.025_6$	.0075

Eisenhauer and Spencer, and Monte Carlo methods. For the first, the source spectrum $S(E)$ photons MeV^{-1} cm^{-2} is needed. For the second, the energy and angular distribution of the radiation incident on the structure $N(E, \Omega, \underline{r})$ photons MeV^{-1} steradian^{-1} cm^{-2} is of more direct use, though the source spectrum $S(E)$ could be used as a starting point.

The Eisenhauer-Spencer methods as presented in references 2, 7, and 9 were used for the comparisons in this report because of their wide availability and acceptance. They do not readily permit use of the energy and angular distributions incident on the structure but assume a plane isotropic source of the 1.12-hr fission products mentioned above. Extension of their calculations to include 3- and 9-day source spectra would be possible but have not been carried out.

Since the barrier-geometry factor methods are given in considerable detail in the above references, particularly reference 2, no detailed discussion will be given here. Appendix A summarizes the procedures which are applicable to our structures, and Appendix B presents sample calculations for a few wall elements.

The PM-100-1 methods treat barrier attenuation separately from geometry attenuation. This treatment is refined by three considerations: (1) wall-scattered radiation is separated from non-wall-scattered, (2) radiation reaching the detector from directions above the horizon is separated from that from directions below, and (3) eccentricity factors are introduced to account for effects of structure shape upon the probability that wall-scattered radiation will reach the detector.

Inside partitions are treated as barriers at a height of 3 ft. No geometry factors are used either in terms of slant thickness or geometry attenuation. This assumes that the angular distribution of the radiation from the exterior barrier is unchanged by the inside partitions. The analysis used here followed this procedure. The lateral extent of inside partitions was acknowledged by use of azimuthal sectors as given in Chapter V of reference 2. The exterior walls were considered to be at their physical height plus 24 ft, the equivalent air layer representing ground roughness.

Eccentricity factors in some cases are ambiguous. Wherever a choice existed, we always took the square configuration rather than a rectangular one.

Instead of treating the structure as a unit our calculations were made for individual external wall elements in order to find which portions of the structures were more transparent to the radiation. The wall elements were generally defined by changes in the barrier thickness, i.e., added thickness introduced by floors, ceilings, and partitions. Each exterior wall of the story in which the detector was located was separated into two elements, the portion above the detector plane and the portion below. Whenever several wall areas were identical in their attenuating properties (this infers that they are symmetrical portions of the structure) they were added azimuthally and considered as a single type of wall element. Finally exposure contributions through the wall elements implicitly assume that all other portions of the structure are totally opaque. When contributions through all wall elements are summed, we obtain the reduction factor for one detector position.

Separate calculations for each wall element (see sample calculations in Appendix B) are somewhat repetitious if only an overall reduction factor is desired. Thus, in routine analysis of structures one would rather choose procedures taken directly from examples given in reference 2.

COMPARISON OF EXPERIMENTAL AND CALCULATED RESULTS

The experimental exposure reduction factors are shown graphically in Fig. 4. We see that differences between the top and middle stories are small. On the other hand the 2 in. of lead upon which each structure sat produced somewhat greater reduction throughout the first story, especially for the thinner walled structures.

The most interesting comparisons of experimental and calculated reduction factors are those representing extreme differences. These extremes consist of compartments designated as A and I, i.e., the top corner compartments and the bottom central-core compartments (see Fig. 3 or insert of Fig. 4). Further comparisons are included for compartments E, those at the center of each side of the structure, and F, the compartment at the center of the structure. Calculations in each case were made for all wall thicknesses used.

Calculations for compartments designated as B, C, D, G, and H were not made as each differed only slightly from that either on the story above or the story below.

Table 3 compares calculated and experimental reduction factors. The calculated values are always higher as indicated by the ratios of calculated to experimental always being greater than unity. These

Table 3

COMPARISON OF CALCULATED AND EXPERIMENTAL REDUCTION FACTORS, D/D_o AND $\tilde{D}/\tilde{D}_o$

Compartment		Nominal Wall Thickness (in.) 1/4	3/8	1/2	3/4	1	1-1/2
A	Calculated	0.304	0.273	0.229	0.184	0.139	0.086
	Experimental	.252	.204	.161	.110	.093	.045
	Calculated / Experimental	1.21	1.34	1.42	1.67	1.48	1.90
E	Calculated	0.246	0.213	0.168	0.124	0.091	0.050
	Experimental	.216	.162	.124	.076	.062	.027
	Calculated / Experimental	1.14	1.31	1.36	1.64	1.47	1.84
F	Calculated	0.219	0.174	0.123	0.071	0.039	0.0144
	Experimental	.183	.122	.080	.038	.029	.0081
	Calculated / Experimental	1.21	1.49	1.56	1.86	1.40	1.79
I	Calculated	0.198	0.169	0.117	0.068	0.040	0.014
	Experimental	.140	.106	.063	.034	.026	.0075
	Calculated / Experimental	1.42	1.60	1.86	2.02	1.55	1.90
F'	Calculated / Experimental	1.35	1.68	1.74	2.01	1.51	1.90
Exposure Period (D + hours)	t_1	95.5	74.5	122.7	74.5	167.6	74.5
	t_2	119.2	91.9	165.6	119.2	261.9	165.6

ratios are shown graphically in Fig. 5 along with the ages of the fission products during the periods of exposure.

The differences between calculations and experiment would be somewhat less if actual mass thicknesses were used instead of effective mass thicknesses. In the calculations all steel thicknesses were converted to effective mass thicknesses by multiplying by 0.931 to adjust them to the same electron density present in concrete, a procedure given in reference 7. In practice it may be preferable not to use this correction.[10,11] For a non-central compartment of the thinnest-walled structure, calculations based upon actual mass thicknesses would yield reduction factors about 3 percent smaller (greater protection) than those given in Table 4. For the other extreme, the centermost compartment of the thickest-walled structure, the calculated reduction factor would become about 20 percent smaller. Such differences are significant and indicate that a revised set of corrections may be needed for converting the shielding effectiveness of various materials to that of concrete.

But the differences are still unexplained. For a given detector position the ratio of the calculated to experimental protection factors should have been unity for all structures provided that the PM-100-1 methods were accurate, the use of effective barrier thicknesses were valid and if only the 1.12-hour fission-product gamma-ray spectrum were encountered. If the ratio varies systematically with wall thickness, one would first suspect the PM-100-1 barrier factors to be incorrect. (The geometrical conditions being fixed imposes a slower variation of geometry factor than barrier factor.) But a different spectrum also will produce a ratio that varies systematically with wall thickness. The question of whether or not the PM-100-1 methods are adequate depends upon whether or not we can ascribe the entire variation shown in Fig. 6 to differences in spectrum.

The variation of protection factor in an underground shelter as a function of age of the fission products is shown in Fig. 3-3 of reference 2. Similar curves are presented in reference 12. Specifically at H + 100 hours and for a barrier thickness of 100 psf (equivalent to about 2.7 in. of steel) these curves indicate that the ratio of the reduction factor at 1.12 hours to that at 100 hours to be about 1.4. Experimental time integrated reduction factors from H + 74.5 to 165.5 hours for compartments I and F having nominal (single) wall thickness of 1-1/2 in. are grossly comparable; however, we find about 80 percent enhancement of protection. This excess not identifiable with spectral changes suggests that the PM-100-1 methods applied to these structures may underestimate protection by as much as 50 percent for total barrier thicknesses up to 120 psf. Perhaps nearly half of

Table 4

CALCULATED VALUES OF D/D_o - COMPARTMENT A

Wall Element	Nominal Wall Thickness (in.)					
	1/4	3/8	1/2	3/4	1	1-1/2
a	0.0021	0.0014	0.0008	0.0003	0.0002	0.0001
b	.0026	.0018	.0012	.0007	.0004	.0001
c	.047	.053	.053	.050	.043	.031
d	.0097	.0092	.0079	.0059	.0039	.0018
e	.0072	.0053	.0034	.0016	.0007	.0002
f	.0344	.0282	.0206	.0127	.0074	.0030
g	.175	.155	.130	.106	.079	.048
h	.0027	.0017	.0009	.0004	.0002	.0000
i	.0230	.0171	.0112	.0063	.0037	.0014
j	.0004	.0002	.0001	.0000	.0000	.0000
Sum	0.304	0.273	0.229	0.184	0.139	0.086

this discrepancy may result from the use of effective barrier thicknesses as indicated above. But this crude comparison at H + 100 hours is for greatly different sheltering conditions; consequently, we can only speculate that a real discrepancy exists.

Two other aspects of Fig. 6 should be noted. If spectral effects dominate the discrepancy between calculated and experimental values, then the discrepancy becomes greater and greater for increasing wall thickness. The trend of the curves bears this out. For wall thickness up to 3/4 in. compartments A and F, representing single wall thicknesses between the detector and the outside, give discrepancies comparable to those for compartments F and I at half the wall thickness (times two for equivalent total thickness). For nominal wall thicknesses of 1 and 1-1/2 in. I and F no longer show greater discrepancies than A. This puzzling observation throws doubt upon any attempt to remove spectral effects quantitatively from the comparisons of calculations and experiment.

An important aspect of Fig. 5 is the trough occurring at 1-in. wall thickness. This results from the penetrating ability and abundance of 1.6 MeV gamma rays from La^{140} during this exposure period.

Compare the intensity spectra shown in Fig. 1. The 1.12-hour spectrum is somewhat harder than that at 9 days; therefore it is quite possible that the trough of Fig. 5 would be deeper if the exposure had been to the 1.12-hour spectrum. If correct, this argument would assign most of any discrepancy to spectral differences. For the 1-in. thickness, perhaps about 15 percent of the discrepancy might be assigned to the use of effective barrier factors.

The foregoing discussion is inconclusive. Unless suitable barrier and geometry attenuation curves are generated for the spectra existing during the exposure periods and additional calculations are made, we cannot claim on the basis of these experiments that the PM-100-1 methods either do or do not predict protection factors accurately in a real fallout field.

Some insight into the relative importance of the various portions of the structure in providing shielding will be considered next, starting with the detector in compartment Type A. Figure 6a gives the exposure contribution in percent from radiation passing through each group of similar wall elements, for each wall thickness. The contributions through structural elements not labeled are assumed to be zero. The contributions through elements designated h and j are small enough to indicate that this assumption introduces no serious error. The percentages given represent the total contribution through symmetrical wall elements and are listed in order of increasing wall thickness.

If we add contributions from elements c and g (to give the portion of the room bounded by a single outside wall) their total becomes:

Wall Thickness (in.)	Relative Dose Contribution (percent)
1/4	73
3/8	76
1/2	80
3/4	85
1	88
1-1/2	92

It is clear that most of the refinements of the PM-100-1 methods for treating floors, ceilings, and inside partitions are overwhelmed. Hence, even if it were concluded that these experiments confirmed the predictions made using PM-100-1, special configurations in which the radiation must arrive by circuitous routes remain essentially untested here. Subsequent experimentation that attempts to test the PM-100-1 methods should be designed carefully so that as few factors as possible are involved.

Figure 6b shows reduction factors as functions of wall thickness for the various wall elements. Implicitly each curve assumes all other elements are totally opaque. The sum of these curves gives the solid curve at the top. The experimental results are included as points. Extrapolation of the experimental and "structure" curves to 0.59 at zero wall thickness reflects the presence of ground roughness and the height of the detector.

The calculated value of D/D_o for each wall element is given in Table 4.

Figures 7a and 7b, 8a and 8b, and 9a and 9b show similar results as given above but for detector positions E, F, and I respectively. Tables 5, 6, and 7 give calculated values of D/D_o.

We saw earlier that radiation through the thinner portions of the structure largely dominated the reduction factor achieved at detector position A. Will this also be true for detector position F, the center

Table 5

CALCULATED VALUES OF D/D_o - COMPARTMENT E

Wall Element	Nominal Wall Thickness (in.)					
	1/4	3/8	1/2	3/4	1	1-1/2
a	0.0025	0.0018	0.0012	0.0005	0.0002	0.0001
b	.0014	.0009	.0006	.0003	.0001	.0000
c	.0014	.0011	.0009	.0005	.0003	.0001
d	.0091	.0081	.0060	.0034	.0019	.0006
e	.0052	.0052	.0044	.0031	.0022	.0009
f	.0097	.0096	.0077	.0059	.0041	.0018
g	.0255	.0260	.0262	.0250	.0225	.0154
h	.0185	.0143	.0090	.0043	.0021	.0006
i	.0326	.0282	.0198	.0125	.0076	.0030
j	.0344	.0294	.0208	.0128	.0078	.0030
k	.0882	.0773	.0649	.0526	.0408	.0240
l	.0075	.0048	.0028	.0013	.0005	.0001
m	.0040	.0025	.0014	.0007	.0003	.0001
n	.0057	.0038	.0026	.0014	.0008	.0003
Sum	0.246	0.213	0.168	0.124	0.091	0.050

Table 6

CALCULATED VALUES OF D/D_o - COMPARTMENT F

Wall Element	Nominal Wall Thickness (in.)					
	1/4	3/8	1/2	3/4	1	1-1/2
a	0.0057	0.0040	0.0027	0.0013	0.0006	0.0001
b	.0061	.0037	.0023	.0008	.0003	.0001
c	.0244	.0226	.0160	.0090	.0051	.0016
d	.0212	.0210	.0176	.0129	.0090	.0040
e	.0781	.0596	.0372	.0180	.0087	.0023
f	.0630	.0585	.0414	.0259	.0159	.0062
g	.0116	.0062	.0036	.0014	.0005	.0001
h	.0108	.0065	.0041	.0019	.0009	.0002
Sum	0.219	0.174	0.123	0.0711	0.0391	0.0144

Table 7

CALCULATED VALUES OF D/D_o - COMPARTMENT I

Wall Element	Nominal Wall Thickness (in.)					
	1/4	3/8	1/2	3/4	1	1-1/2
a	0.0053	0.0039	0.0026	0.0013	0.0006	0.0001
b	.0056	.0036	.0021	.0008	.0003	.0001
c	.0244	.0216	.0158	.0090	.0049	.0015
d	.0212	.0202	.0175	.0129	.0086	.0040
e	.0781	.0573	.0368	.0180	.0084	.0022
f	.0630	.0560	.0410	.0259	.0152	.0062
Sum	0.197	0.162	0.116	0.0679	0.0377	0.0141

of the middle story, where alternate pathways traverse comparable thicknesses? The percent exposure contributions through walls of the second story are given in Table 8.

When the walls are thin, radiation through walls of the corner compartments contribute nearly half the total exposure even though it must pass through two interior walls. When the walls have a thickness of 20 psf (1/2 in. of steel) or more, radiation through the side-compartment walls contribute more than half the total exposure. Radiation through the second-story walls but from below the detector plane produced about 60 percent of the total exposure for all wall thicknesses used. These calculations suggest that rule-of-thumb procedures might be developed which could predict reduction factors for simple structures fairly well. The presence of windows might even simplify the procedure in some cases.

The fifth column of Table 8 shows that no other stories contribute materially to the total exposure. Multiplying the results for the second story by 1.1 would give a good prediction for the structure over the range of wall thicknesses used.

The above discussion is based upon the validity of PM-100-1 calculations, but the general conclusions may be correct even if deficiencies do show up in the calculations. The comparison of calculated and experimental results further suggest a deficiency which will be discussed next.

The calculations for compartments F and I were identical except that in the case of I we assumed that the lead shields upon which the structures sat prevented any radiation from reaching the detector after passing through the floor of the first story.* If we compare the ratios of calculated to experimental reduction factors as given in Table 3 we find the ratios for compartment I to be consistently greater than for F. The differences in ratios are even greater than shown since those for I will tend to be low at greater wall thicknesses where 2 in. of lead no longer is thick relative to 2 or 3 in. of steel.

---

*Strictly speaking, the calculations are not identical since there is a height difference. This difference was 10 in. at an effective height of 28 ft and can be read into the PM-100-1 charts only if much care is taken. That this height difference can be neglected is borne out by the small differences observed between the second and third stories of Fig. 5, part of which is attributable to skyshine radiation.

Table 8

EXPOSURE CONTRIBUTIONS TO DETECTOR POSITION F THROUGH SECOND STORY WALLS
(PM-100-1 Calculations)

Wall Thickness (in.)	Radiation Through Side Compartments (d + f) (%)	Radiation Through Corner Compartments (c + e) (%)	Radiation From Below Detector (e + f) (%)	Total Radiation Through Second Story Walls (c + d + e + f) (%)
1/4	38	46	64	85
3/8	44	45	65	89
1/2	47	43	63	90
3/4	54	38	62	92
1	61	34	60	94
1-1/2	71	27	59	97

Since no differences in the ratios should exist between F and I if the calculational method is satisfactory, we conclude that the PM-100-1 method of treating radiation coming through the walls and ceiling of the story below underestimates the exposure considerably. Floor barrier factors are obtained by using the barrier factor curve for contaminated roofs, a scheme which makes a floor much more efficient in attenuating radiation than a wall or inside partition. The angular distribution of radiation at the bottom surface of a floor is different from that for interior walls in that a greater portion of the radiation will be at or near grazing incidence; consequently, the use of a barrier factor curve that gives greater attenuation would seem to be justified. Since experiment shows less attenuation than do the calculations, let us consider the conditions which give the least attenuation by the floor. This will occur if the floor thickness is added to the exterior wall thickness and a wall barrier factor for the combined thickness is obtained from reference 2 (chart 1, case 2). Interior walls were treated as before. Thus, the total barrier attenuation for a floor, an exterior and two interior walls in a structure at height H would be

$$B_w\left[(X_e + X_f),\ H\right] B_w(X_i, 3') \ B_w(X_i, 3')$$

instead of

$$B_w(X_e, H)\ B_o(X_f)\ B_w(X_i, 3')\ B_w(X_i, 3').$$

When the reduction factors for F are calculated in this manner and compared with experimental results, the ratios agree better with those obtained at detector position I. These ratios are shown as F' at the bottom of Table 3.

The above procedure is not intended as a substitution for the present PM-100-1 procedure. It rather indicates that a drastic modification is needed if floor penetration is to be handled satisfactorily.

CONCLUSIONS AND RECOMMENDATIONS

1. Evidence is presented which attribute most of the differences between calculated and experimental reduction factors to differences in the gamma-ray spectra. Other evidence suggests that the PM-100-1 calculational methods may be partly at fault.

2. The experimental data were generally accurate and provide valuable information for testing calculations. Conceivably curves could be generated for the gamma-ray spectra that were encountered during the experiments and a more valid test of the PM-100-1 methods could be made.

3. Refinements of the PM-100-1 procedures are masked by the preponderant amount of the dose that results from radiation coming through the thinnest paths. In the design of further experiments much care should be taken to isolate each factor to be tested. In those cases where this is not possible to do experimentally, reliance should be made upon Monte Carlo calculations.

4. The barrier factors used for floors appear to give too much attenuation. Additional thought and perhaps experiments should be given to improving the treatment of floors, especially when they are thin.

APPENDIX A

PM-100-1 Methods

We consider the reduction factor as applied to the structures of this report.

$$\tilde{R} = \sum_{\text{elements}} A_z(\phi)\, G(X,\omega,H,E) \prod B(X,H)$$

where B is a barrier factor which is read from charts provided in reference 2. Particularly, it will be $B_w(X,H)$, $B_o'(X_o)$, or $B_o(X_f)$ for a wall, a ceiling, or a floor respectively. The X's represent effective mass thicknesses in concrete equivalent lbs/ft^2 and H represents the effective height of the detector $d + \tau$, where d is the physical height and τ is the air-equivalent overlayer thickness which corrects for ground roughness. The symbol $\prod$ indicates multiplication together of the appropriate barrier factors, one for the exterior structure element and one for each additional barrier interposed between that element and the detector.

The factors $A_z(\phi)\, G(X,\omega,H,E)$ account for geometrical effects of the structure upon the probability that radiation will reach the detector. Because of the many shapes that structures may take, this geometry dependence is complicated. The PM-100-1 methods transform the structure into an equivalent cylinder appropriate to the structural element being evaluated; accordingly, a cylindrical coordinate system is used. The factor A_z accounts for the azimuthal extent of the element, and the factor G accounts for its polar extent (by means of the solid angle parameter ω which is related to the polar angle θ through the relation $\omega = 1 - \cos\theta$).

The X dependence of G accounts for the different angular distributions of the scattered and unscattered radiation. The dependence of G upon the eccentricity factor E accounts for the effect of structure shape, specifically the ratio of width to length, upon the likelihood that wall-scattered radiation will strike the detector.

G dependence upon radiation arriving at the detector from above the detector plane combines both radiation scattered from the ceiling and from the atmosphere (skyshine). It also includes a wall-scattered component which is considered in all respects identical to a wall-scattered component arriving from below the detector plane. G dependence upon radiation from below the detector plane also includes the unscattered radiation from the fallout field. These various geometrical routes are mutually exclusive and consequently are additive. The wall-scattered radiation, both from above and below the detector plane, must be corrected by the eccentricity factor E before it can be added to the other geometry components.

The factor G is applied only to exterior wall elements. The assumption is that the angular distribution of radiation that has penetrated the outside walls is unaltered by internal barriers. Interior walls, ceilings, and floors merely define the azimuthal and polar limits of the wall elements. The use of B_o and B_o' instead of B_w as barrier factors for floors and ceilings does introduce geometrical effects into their attenuating efficiency, but the factor G remains unchanged. The barrier factor B_w for an interior wall is considered to be the same as that of an exterior wall at a height of 3 ft. This tacitly assumes that the angular distribution of the incident radiation upon one is equivalent in a practical sense to that upon the other regardless of the orientation of the interior (vertical) wall.

APPENDIX B

Sample Calculations

Three sample calculations, Tables B-1, B-2, and B-3, are for greatly dissimilar wall elements. The purposes of the calculations are (1) to indicate the magnitudes of the arguments and functions as applied to particular shielding elements, and (2) to present typical but specific calculations for the structures we used.

On each calculation sheet are plan, elevation, and side views of the structure which identify the detector position and the wall elements being treated. The equation at the top of each sheet includes only those factors which enter into the particular calculation. For detailed procedures, the nomenclature, and the charts of the functions the reader should use reference 2.

In each case the reduction factor is the exposure (relative to D_0) resulting from radiation passing through all structural elements which are symmetrically located with respect to the detector. All other elements are considered totally opaque. Calculation of the exposure from radiation through all parts of the structure is accomplished by summing over all structural elements.

The circled numbers refer to chart numbers in reference 2.

Table B-4 gives the effective barrier thicknesses used for the calculations. As mentioned in the text, these values have been adjusted to have the same electron density as concrete per $lb\text{-}ft^{-2}$. References 10 and 11 suggest that for iron actual values of mass thickness may give better estimates of attenuation than these adjusted values.

Table B-1

CALCULATION OF RELATIVE EXPOSURE $(D/D_o)_{A,e}$ AT DETECTOR POSITION A FROM RADIATION THROUGH ELEMENTS e

$$A_z \left\{ \left[G_s(\omega) - G_s(\omega') \right] S_w(X_e)\, E(e) + \left[G_d(\omega,H) - G_d(\omega',H) \right] \left[1 - S_w(X_e) \right] \right\} x$$

$$B_w(X_e,H)\, B_w(X_i',3')\, B_w(X_i',3')$$

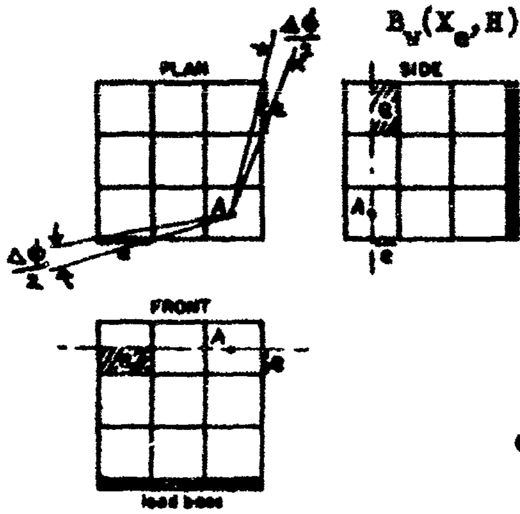

	INNER LIMIT	OUTER LIMIT		
e	0.2	0.2		
n	0	0.2		
ω	1.00	0.49_5	3	E (0.2) = 1.18 (8)
$G_s(\omega)$	0	0.38_0	5	ΔG_s = 0.38_0
$G_d(\omega, 3')$	0	0.60_5	6	ΔG_d = 0.60_5

$A_z = \Delta\phi/2\pi$
$= \frac{2}{2\pi}\left[\frac{\pi}{4} - \tan^{-1}\frac{1}{3} - \tan^{-1}\frac{1}{3}\right]$
$= 0.040_4$

DESIGNATOR	CHART	NOMINAL WALL THICKNESS (inch)					
		$\frac{1}{4}$	$\frac{3}{8}$	$\frac{1}{2}$	$\frac{3}{4}$	1	$1\frac{1}{2}$
$S_w(X_e)$	7	0.20	0.26	0.34	0.43	0.51	0.61
$\Delta G_s\, E\, S_w$		.089	.117	.153	.193	.229	.274
$1 - S_w(X_e)$	7	0.80	0.74	0.66	0.57	0.49	0.39
$\Delta G_d[1 - S_w]$		.484	.447	.399	.345	.296	.236
$\Delta G_s\, E\, S_w + \Delta G\, [1 - S_w] = G$		.573	.564	.552	.538	.525	.510
$B_w(X_e, 29')$	2	.50	.46	.39	.32	.24	.15
$B_w(X_i', 3')$	1(2)	.79	.71	.62	.48	.38	.25
$B_w(X_i', 3')$	"	.79	.71	.62	.48	.38	.25
~~B (X ,)~~							
$B_w(X_e, 29')\, [B_w(X_i,3')]^2 = B$		.312	.232	$.15_0$	.074	.035	.0094
$A_z\, G\, B$		0.0072	.0053	.0034	.0016	.00073	.0002

Table B-2

CALCULATION OF RELATIVE EXPOSURE $(D/D_o)_{E,m}$ AT DETECTOR POSITION E FROM RADIATION THROUGH ELEMENTS m

$$A_z\left\{\left[G_s(\omega)-G_s(\omega')\right]\,S_w(X_e)E(e)+\left[G_d(\omega,H)-G_d(\omega',H)\right]\left[1-S_w(X_e)\right]\right\}\times$$

$$B_w(X_e,H)\;B_w(X_i',3')\;B_o(X_f)$$

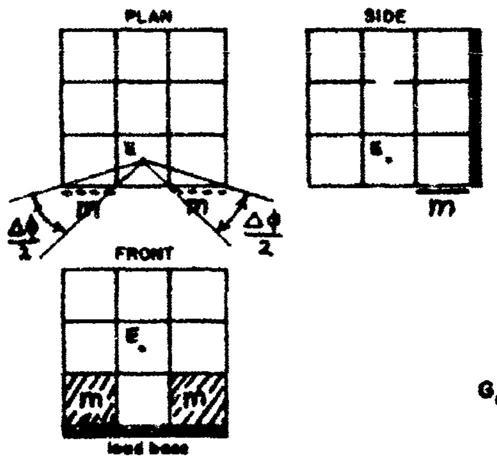

	INNER LIMIT	OUTER LIMIT		
e	1/3	1/3		
n	1	1/3		
ω	0.72	0.48	3	$E(1/3) = 1.27$ 8
$G_s(\omega)$	0.38_5	0.26_6	5	$\Delta G_s = 0.119$
$G_d(\omega, 28')$	0.62	0.42	6	$\Delta G_d = 0.20$

$A_z = \Delta\phi/2\pi$

$= \dfrac{2\tan^{-1}3 - \frac{\pi}{2}}{2\pi}$

$= 0.1476$

DESIGNATOR	CHART	NOMINAL WALL THICKNESS (inch)					
		1/4	3/8	1/2	3/4	1	1 1/2
$S_w(X_e)$	7	0.20	0.26	0.34	0.43	0.51	0.61
$\Delta G_s\, E\, S_w$		0.030	0.039	0.051	0.065	0.077	0.091
$1-S_w(X_e)$	7	0.80	0.74	0.66	0.57	0.49	0.39
$\Delta G_d\left[1-S_w\right]$		0.160	0.14_8	0.132	0.114	0.098	0.078
$\Delta G_s\, E\, S_w + \Delta G\left[1-S_w\right] = G$		0.19_0	0.18_7	0.18_3	0.17_9	0.17_5	0.17_0
$B_w(X_e, 28')$	2	0.52	0.49	0.40	0.33	0.26	0.17
$B_w(X_i, 3')$	I(2)	0.80	0.72	0.63	0.49	0.38	0.25
$B_o(X_f, -)$	I(1)	0.34	0.26	0.21	0.15_2	0.11_3	0.067
~~$B\ (X\ ,\ )$~~							
$B_w(X_e, 28')\cdot B_w\cdot B_o = B$		0.14_1	0.092	0.053	0.024_6	0.010_2	0.0028
$A_z\, G\, B$		0.0040	0.0025	0.0014	0.0007	0.0003	0.0001

Table B-3

CALCULATION OF RELATIVE EXPOSURE $(D/D_o)_{F,c}$ AT DETECTOR POSITION F FROM RADIATION THROUGH ELEMENTS c

$$A_2\left\{\left[G_s(\omega)-G_s(\omega')\right] S_w(X_e)\, E(e) + \left[G_d(\omega)-G_d(\omega')\right]\left[1-S_w(X_e)\right]\right\} \times B_w(X_e,H)\, B_w(X_i,3')\, B_w(X_i',3')$$

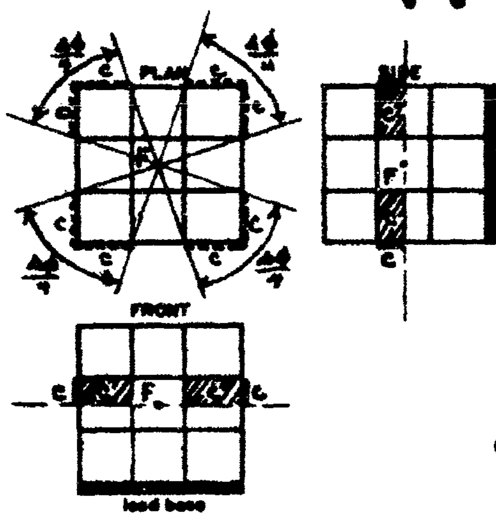

	INNER LIMIT	OUTER LIMIT	
e	1	1	
n	1/3	0	
ω	0.71	1.0	(3)
$G_s(\omega)$	0.273	0	(5)
$G_d(\omega,n)$	0.068	0	(6)

$A_2 = \Delta\phi/2\pi = \frac{8 \times \tan^{-1}\frac{1}{2}}{2\pi} = 0.591$

E(1) = 1.41 (8)

ΔG_s = 0.273

ΔG_d = 0.068

DESIGNATOR	CHART	NOMINAL WALL THICKNESS (inch)					
		1/4	3/8	1/2	3/4	1	1 1/2
$S_w(X_e)$	(7)	0.20	0.26	0.34	0.43	0.51	0.61
$\Delta G_s E S_w$		0.077	0.100	0.131	0.166	0.197	0.236
$1-S_w(X_e)$	(7)	0.80	0.74	0.66	0.57	0.49	0.39
$\Delta G_d[1-S_w]$		0.054	0.050	0.045	0.039	0.033	0.026
$\Delta G_s E S_w + \Delta G\,[1-S_w] = G$		0.131	0.150	0.176	0.205	0.230	0.262
$B_w(X_e, 28')$	(2)	0.50	0.48	0.395	0.32	0.25	0.16
$B_w(X_i, 3')$	(16)	0.79	0.71	0.62	0.48	0.38	0.25
$B_w(X_i', 3')$	(16)	0.79	0.71	0.62	0.48	0.38	0.25
~~B (X ,)~~							
$B_w(X_e, 28')\,[B_w(X_i,3')]^2 = B$		0.312	0.242	0.153	0.074	0.036	0.010
$A_2 G B$		0.0249	0.0216	0.0159	0.0090	0.0049	0.0015

Table B-4

EFFECTIVE BARRIER THICKNESSES

Nominal (in.)	Measured and Adjusted Wall Thicknesses (psf)	
	Exterior	Interior
1/4	9.2	8.8
3/8	12.9	13.6
1/2	19.2	18.4
3/4	27.8	28.4
1	37.5	38.5
1-1/2	56.5	56.7

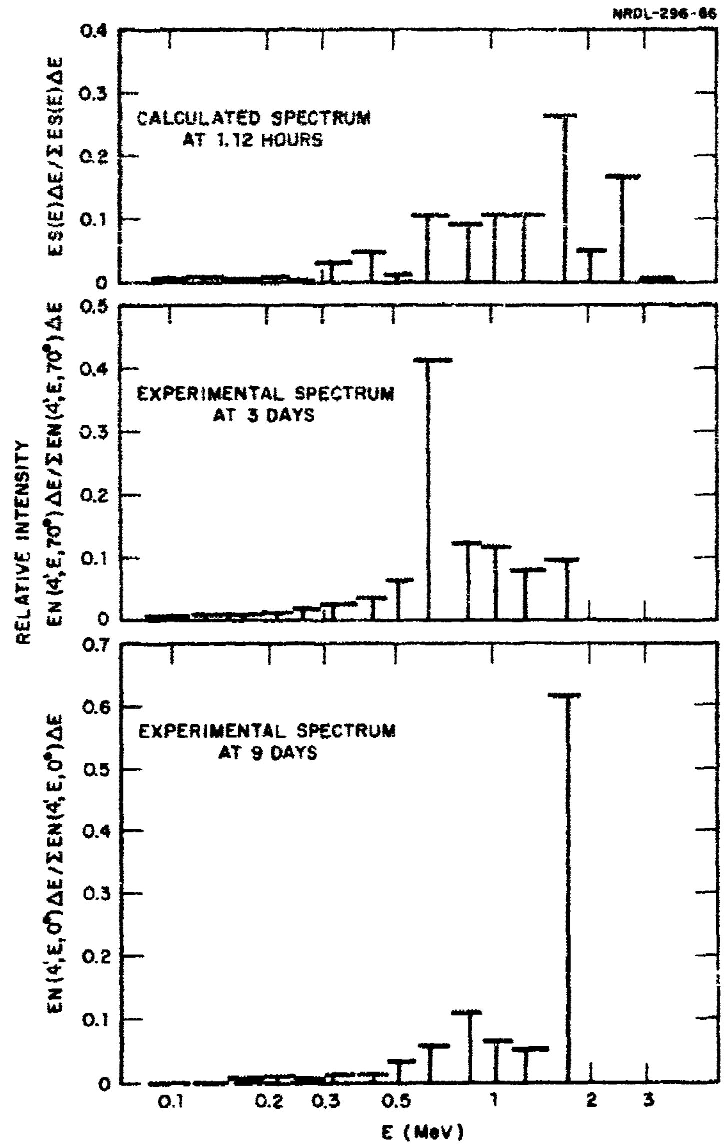

Fig. 1 Gamma-ray relative intensities from fission products at 1.12 hours, 3 days and 9 days. The horizontal bars indicate the width of each energy interval. The vertical bars represent the total intensity within the energy interval and are at the energies that were assumed for the calculation of intensity. Values of S(E) for the 1.12 hour spectrum were taken from Table 4 of reference 5.

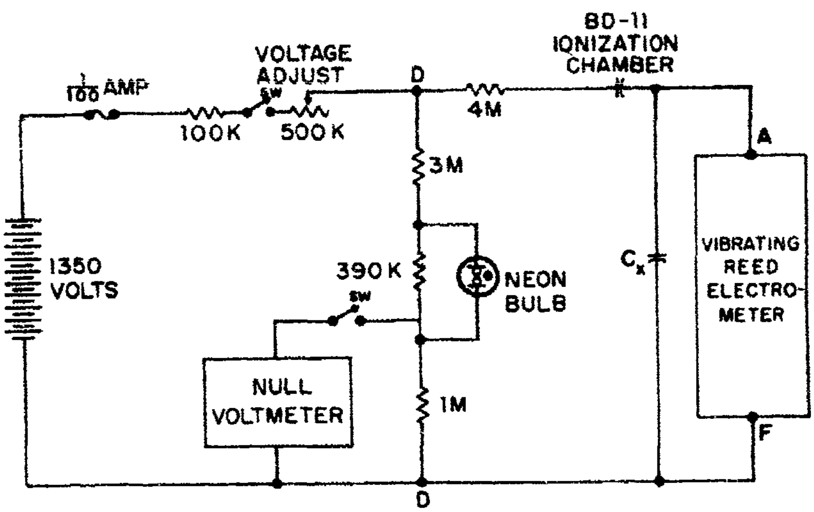

Fig. 2 Charging-reasing circuit for ionization chambers. This system extended the exposure range of BD-11 ionization chambers by a factor of four.

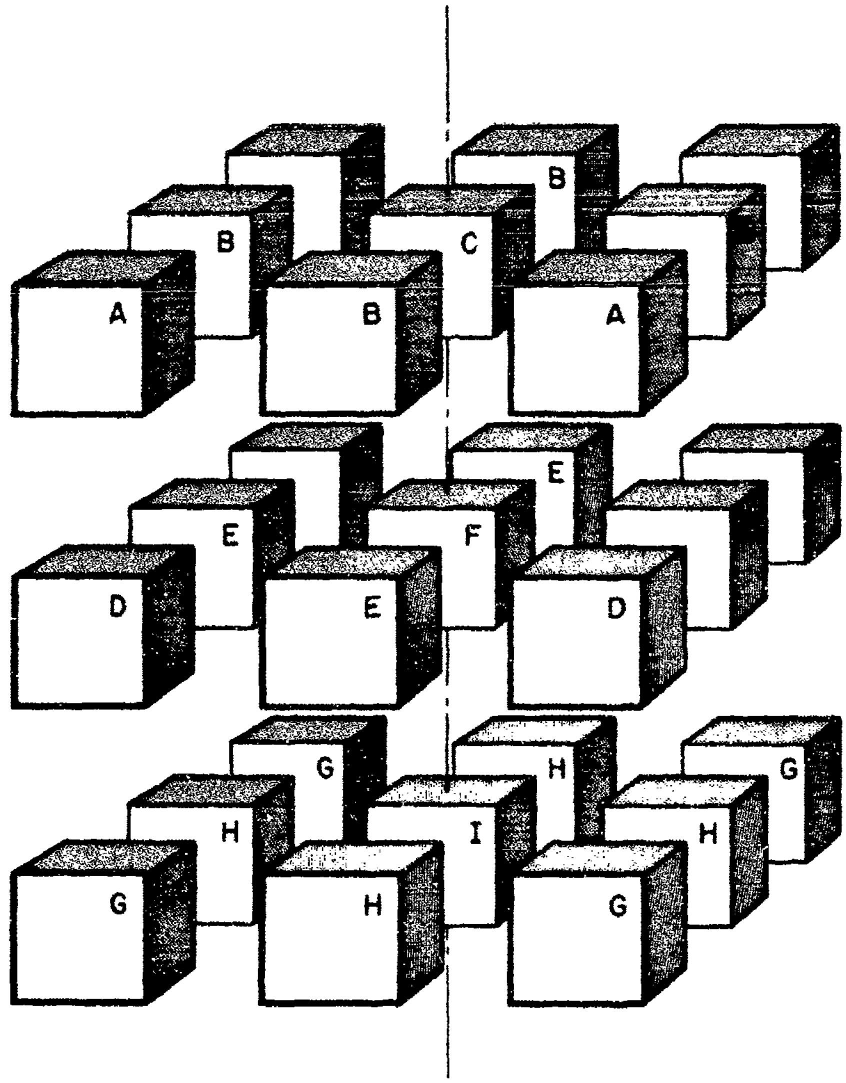

Fig. 3 Compartment designations. Exploded view of structure shows individual compartments. For each compartment the walls that made up the outside surface when the structure was assembled were twice as thick as the inside walls. Thus, when assembled together, the total wall thicknesses exterior and interior were uniformly thick.

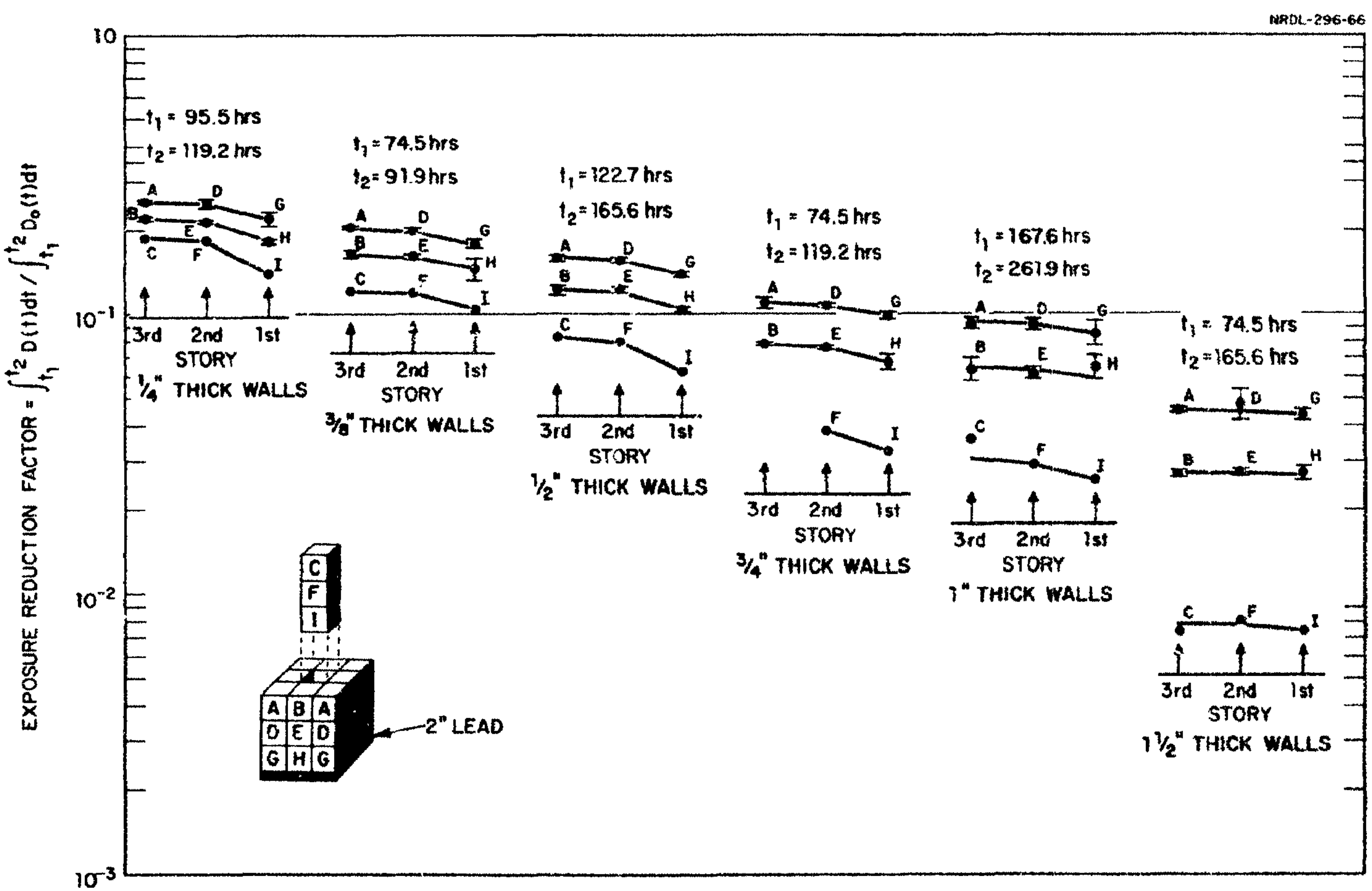

Fig. 4 Exposure reduction factors within six structures of different wall thickness. Reduction factors for symmetrically located compartments were averaged and have been plotted with error bars to show standard deviations. D is the exposure rate within a compartment, D_o is the exterior free field exposure rate corrected for ground roughness equivalent to 24 ft of STP air.

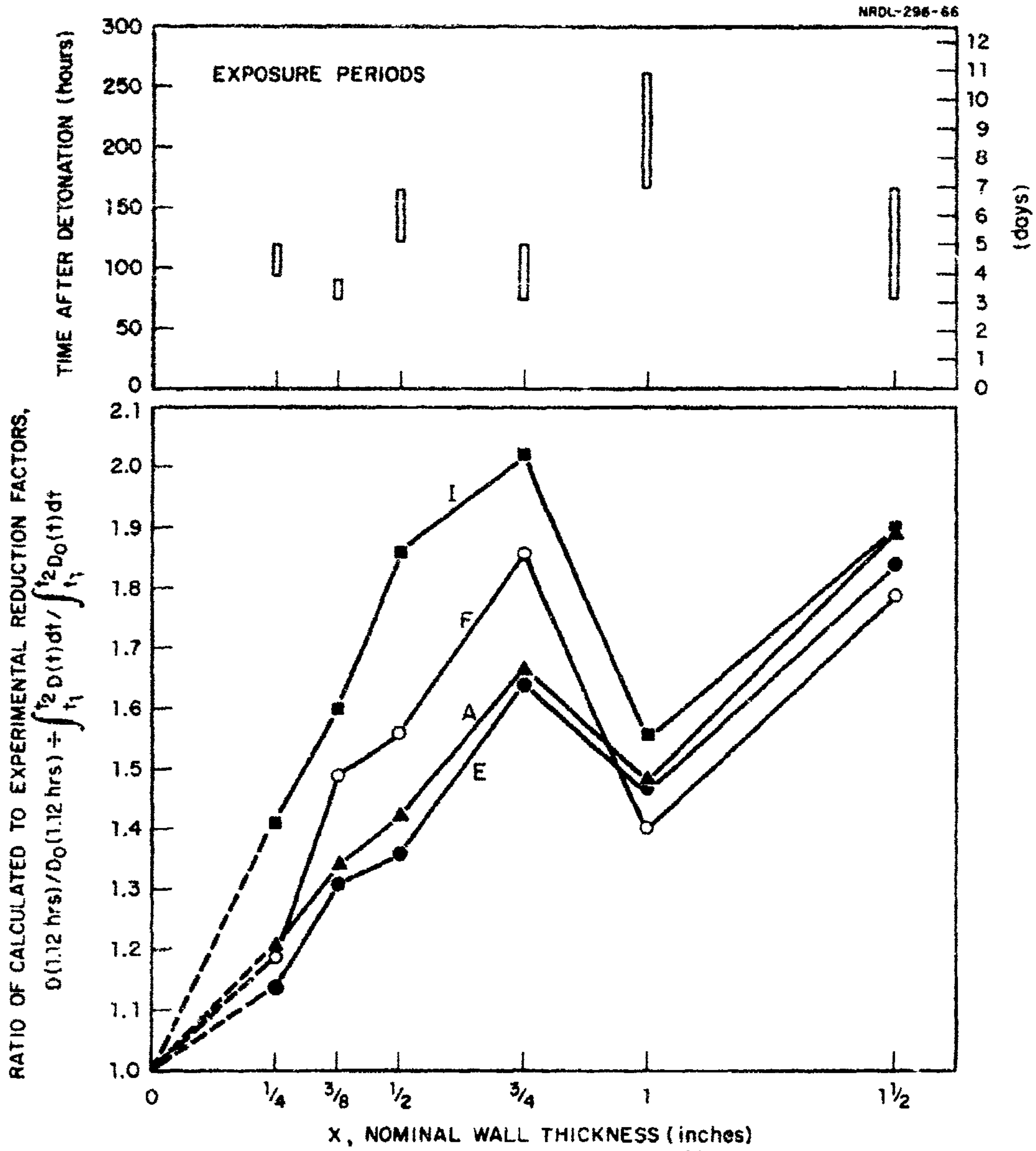

Fig. 5 Comparisons of calculated and experimental reduction factors. The exposure period for each structure is shown directly above the plotted points for that structure. D is the exposure rate within a compartment. D_0 is the free-field dose rate at 3 ft above a smooth plane.

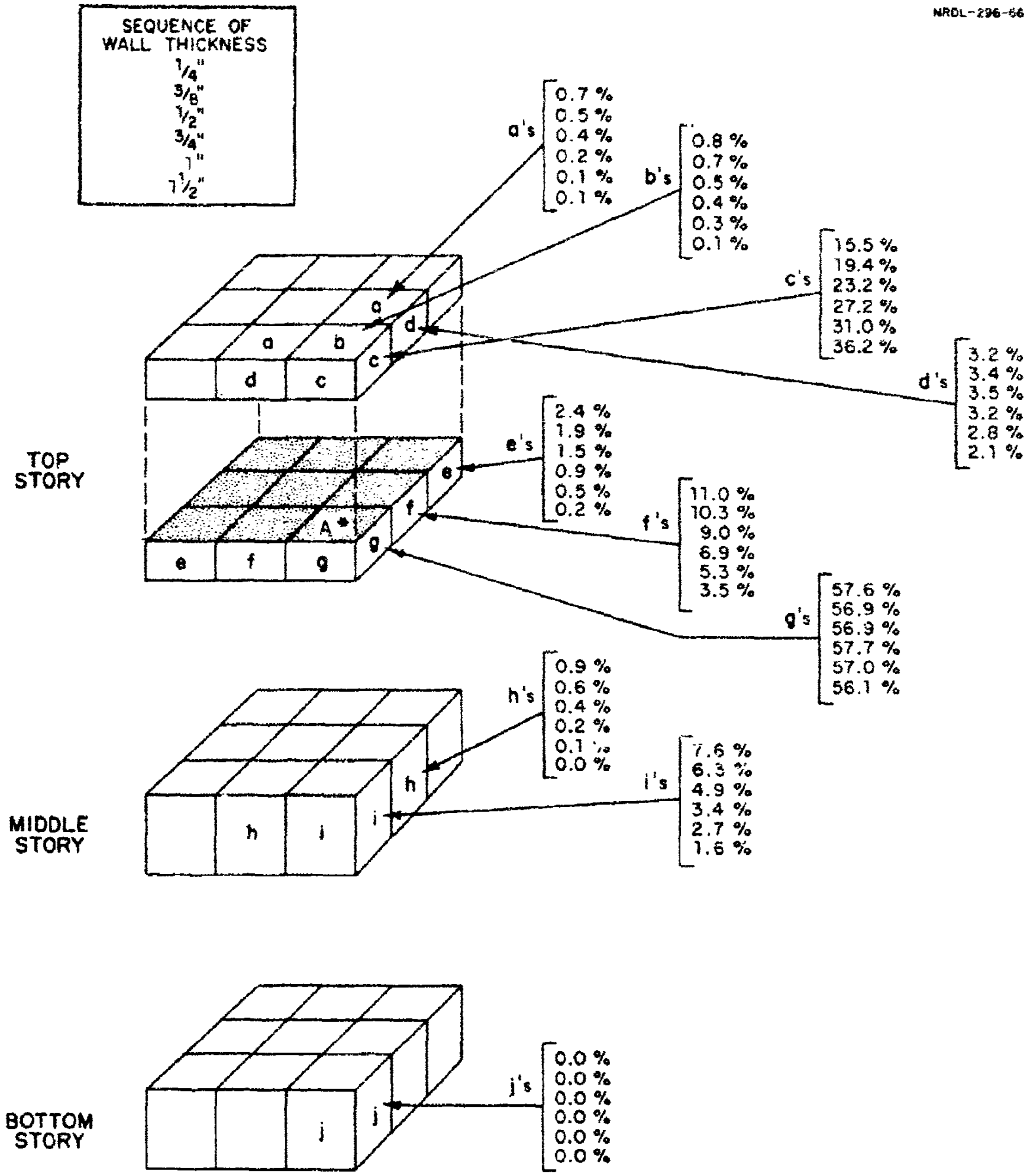

Fig. 6a Percent exposure contribution of symmetrical wall elements to detector position A. The contributions are listed for the six structures in order of increasing wall thickness. These were calculated using PM-100-1 methods.

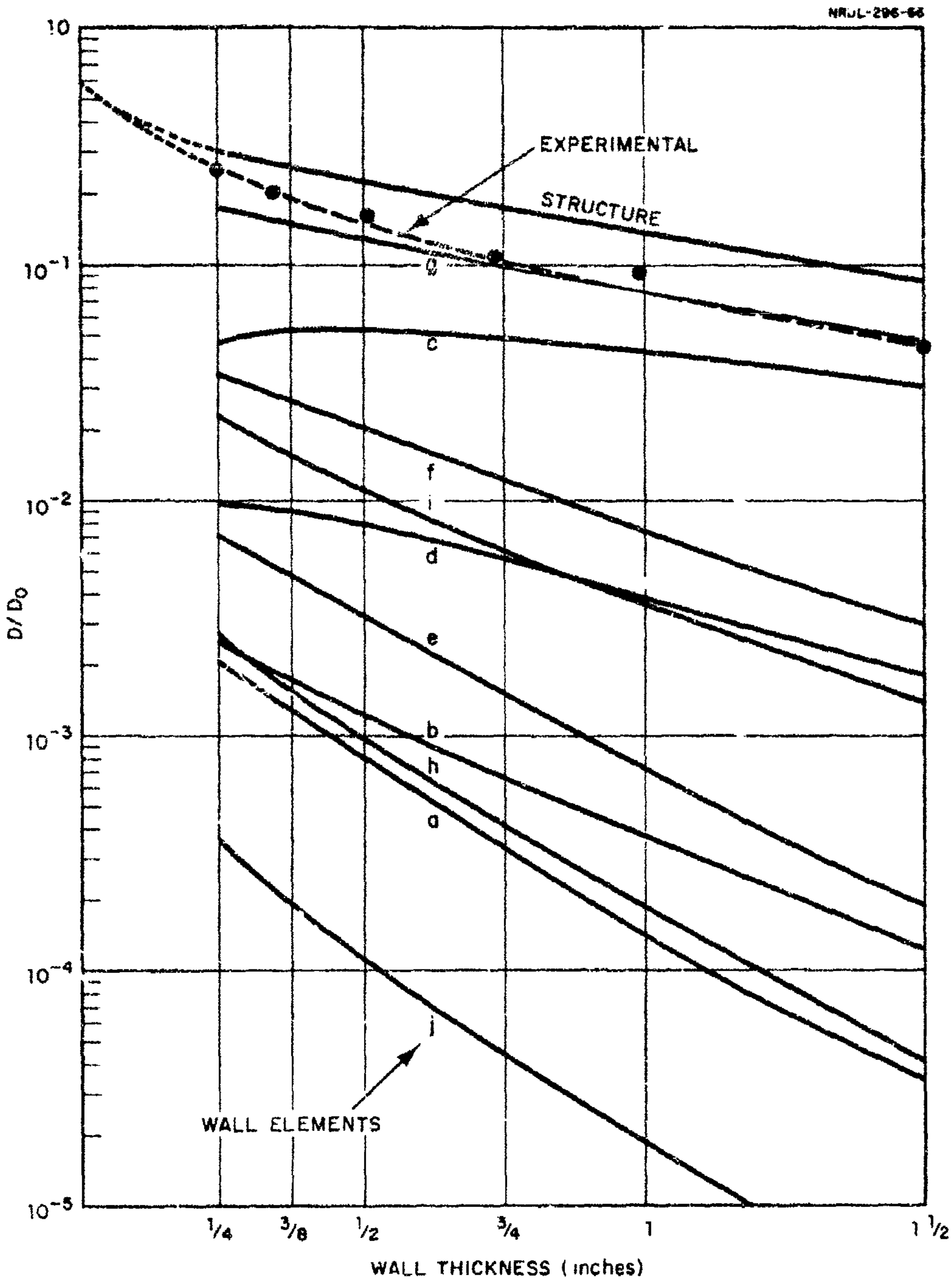

Fig. 6b Calculated exposure contributions through wall elements to detector position A. Letters for each curve are identified in Fig. 6a.

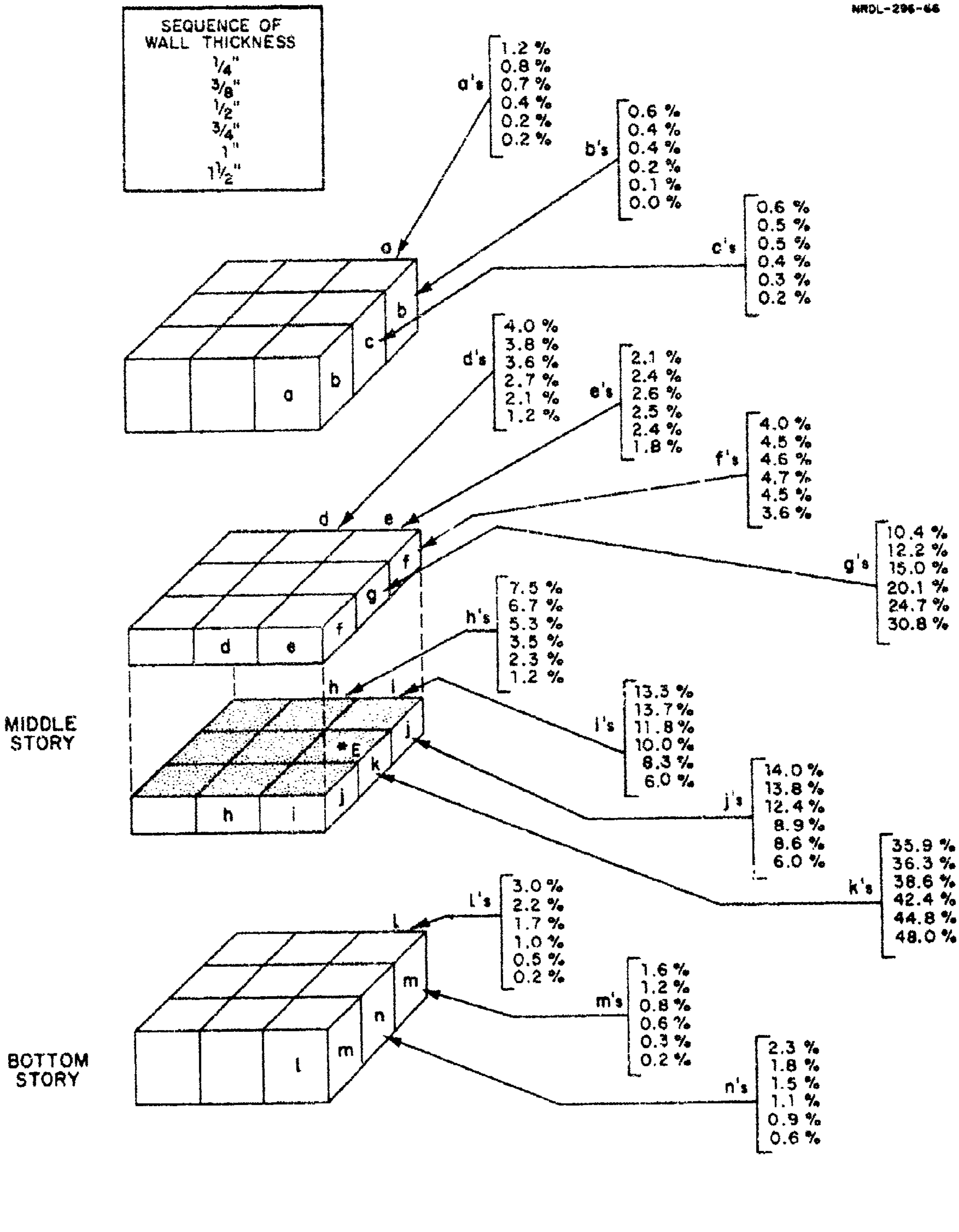

Fig. 7a Percent exposure contribution of symmetrical wall elements to detector position E. The contributions are listed for the six structures in order of increasing wall thickness. These were calculated using PM-100-1 methods.

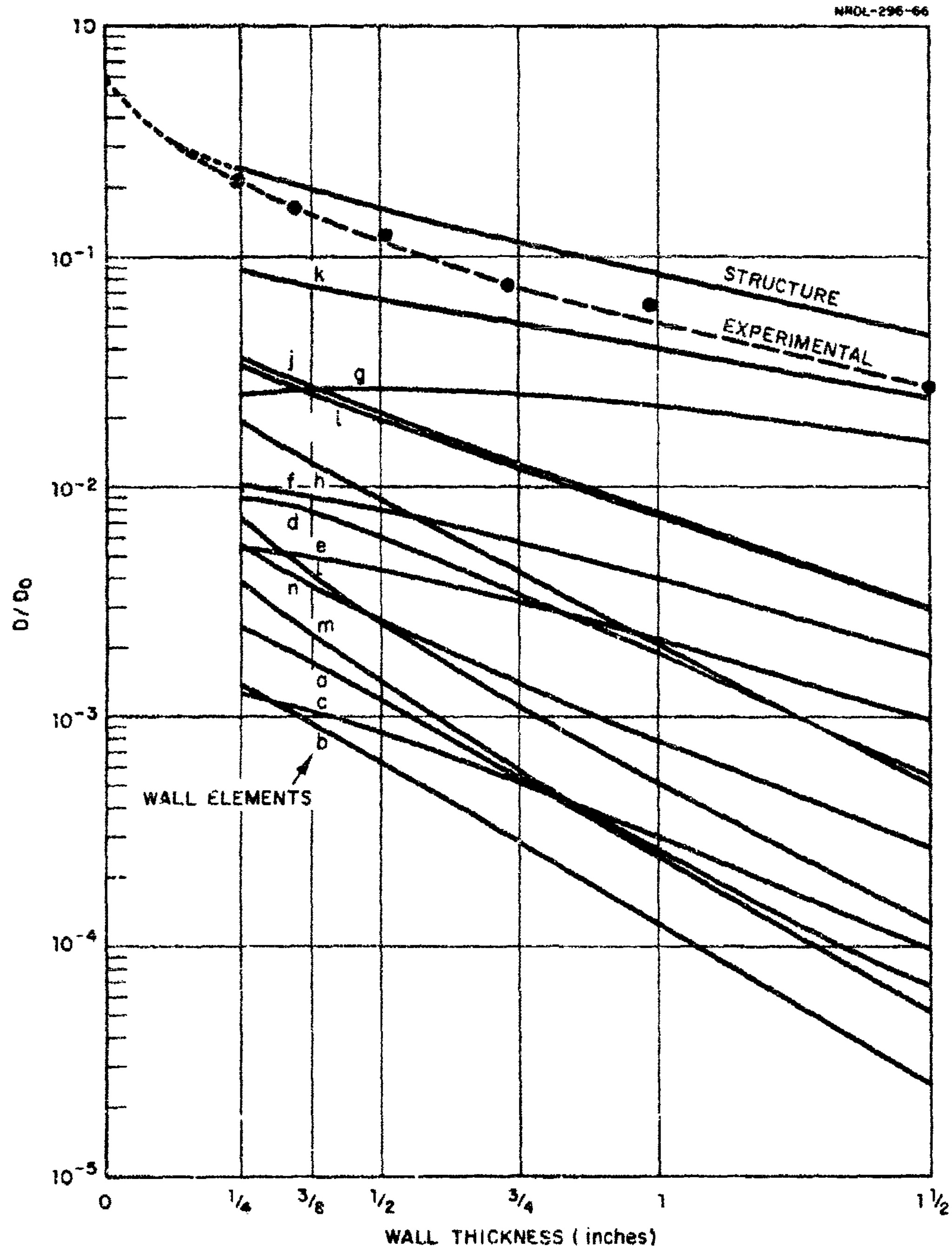

Fig. 7b Calculated exposure contributions through wall elements to detector position E. Letters for each curve are identified in Fig. 6a.

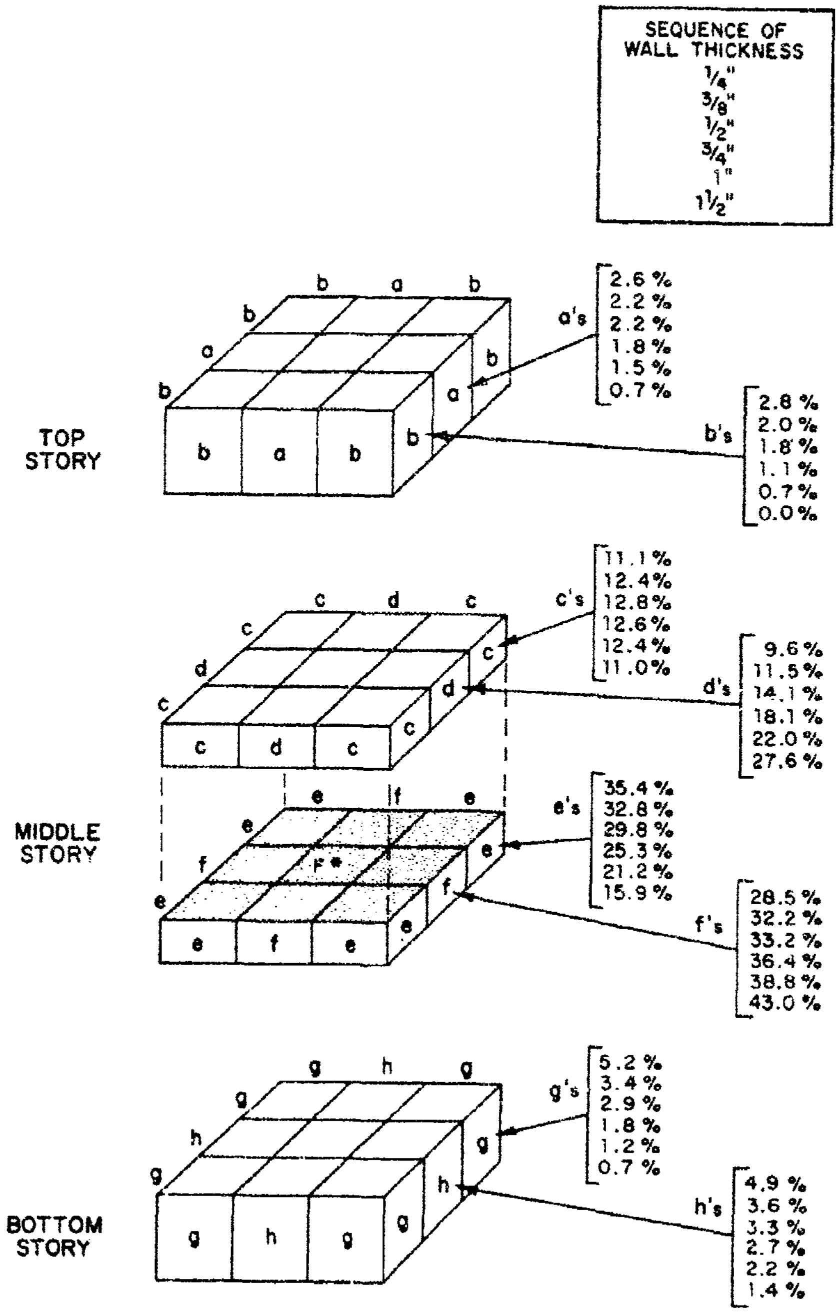

Fig. 8a Percent exposure contribution of symmetrical wall elements to detector position F. The contributions are listed for the six structures in order of increasing wall thickness. These were calculated using PM-100-1 methods.

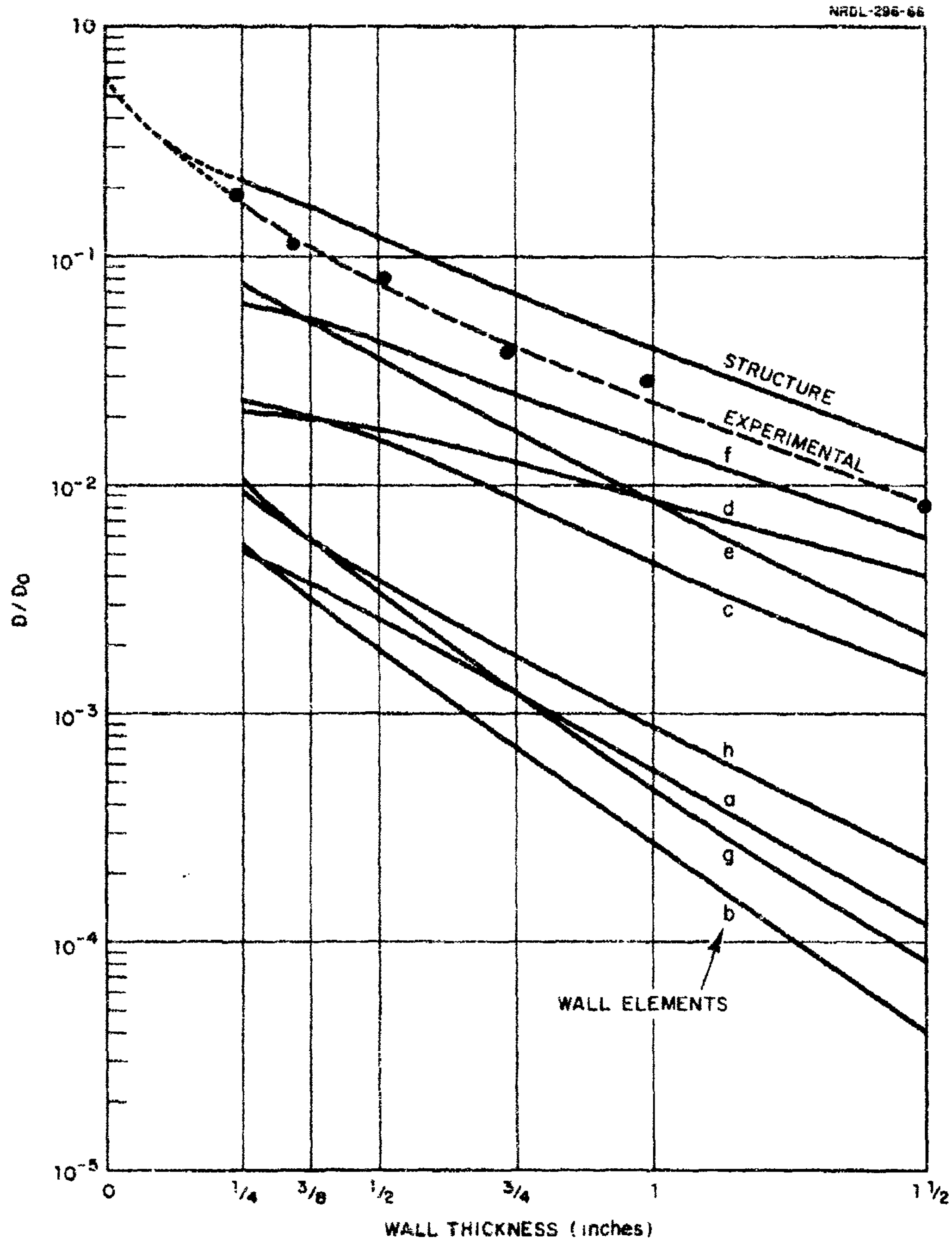

Fig. 8b Calculated exposure contributions through wall elements to detector position F. Letters for each curve are identified in Fig. 6a.

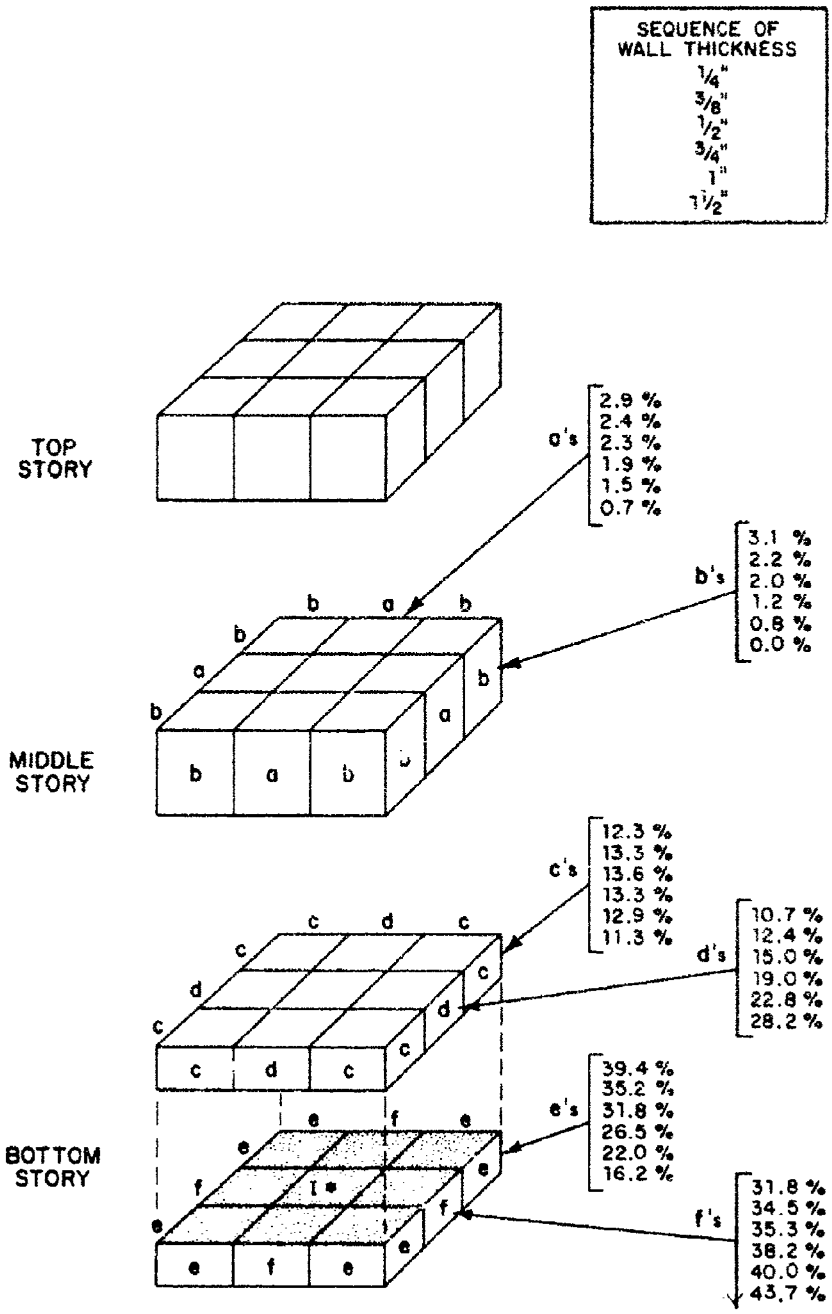

Fig. 9a Percent exposure contribution of symmetrical wall elements to detector position I. The contributions are listed for the six structures in order of increasing wall thickness. These were calculated using PM-100-1 methods.

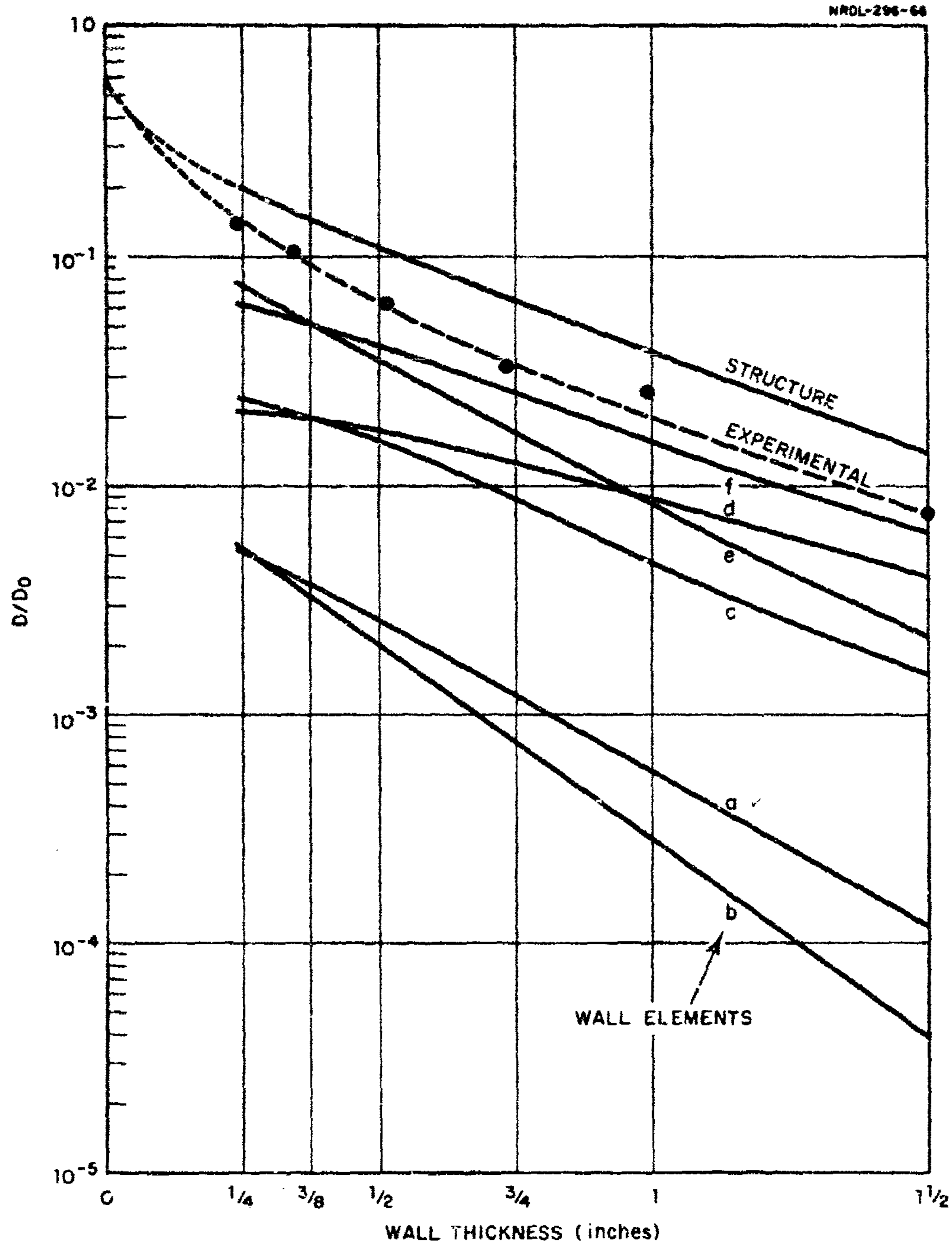

Fig. 9b Calculated exposure contributions through wall elements to detector position I. Letters for each curve are identified in Fig. 6a.

REFERENCES

1. Shumway, B. W., Tomoeda, S., and Frank, A. L., "Shielding Effectiveness of Compartmented Structures in a Fallout Field (U)," POR-2220, Operation SUNBEAM, Shot Small Boy, Project 2.14 (January 1963). OFFICIAL USE ONLY.

2. "Design and Review of Structures for Protection from Fallout Gamma Radiation," PM-100-1 Interim Edition, Department of Defense, Office of Civil Defense (February 1965).

3. Miller, C. F., "Gamma Decay of Fission Products from the Slow-Neutron Fission of U^{235}," USNRDL-TR-187, 11 July 1957 (UNCL).

4. Frank, A. L. and Taylor, R. A., "Gamma Radiation Characteristics - Angular Distribution Over a Desert Terrain Fallout Field," USNRDL-TR-856, 11 June 1965 (UNCL).

5. Nelms, Ann T. and Cooper, J. W., "U^{235} Fission Product Decay Spectra at Various Times After Fission," Health Physics 1, 427-441 (1958).

6. Bigger, M. M., Rinnert, H. R., and Zagorites, H. A., "Shipboard Radiation from Underwater Bursts (U)," WT-1619, 24 March 1961 (CONF).

7. Spencer, L. V., "Structure Shielding Against Fallout Radiation from Nuclear Weapons," National Bureau of Standards Monograph 42, 1 June 1962.

8. Alpen, E. L., "Radiological Hazard Evaluation - A Critical Review of Present Concepts and a New Approach Thereto," USNRDL-TR-186, 22 October 1957 (UNCL).

9. Eisenhauer, Charles, "An Engineering Method for Calculating Protection Afforded by Structures Against Fallout Radiation," National Bureau of Standards Monograph 76, 2 July 1964, Professional Manual PM-100-1, Supplement No. 1 (January 1964).

10. Schmoke, Murray A., and Rexroad, Ralph E., "Attenuation of Simulated Fallout Radiation by the Roof of a Concrete Blockhouse," NDL-TR-6, (August 1961).

REFERENCES (contd.)

11. Clifford, C.E., "Use of Models for Gamma Shielding Studies," DRCL Report No. 364 (February 1962).

12. Donovan, L. K., "Dose Attenuation Factors for Concrete Slab Shields Covered with Fallout as a Function of Time After Fission," NRDL-OCDM R and L No. 110, pp. 211-222, 31 October - 1 November 1960.

INITIAL DISTRIBUTION

Copies	
	NAVY
2	Commander, Naval Ship Systems Command (SHIPS 2021)
1	Commander, Naval Ship Systems Command (SHIPS 20)
1	Commander, Naval Ship Systems Command (SHIPS 03541)
1	Commander, Naval Ship Engineering Center (Code 6423)
1	Chief, Bureau of Medicine and Surgery
1	Commander, Naval Ordnance Systems Command (ORD 034)
1	Commander, Naval Supply Systems Command (Code 0611C)
1	Commander, Naval Facilities Engineering Command (Code 03)
1	Chief of Naval Personnel (Pers M12)
1	Chief of Naval Research (Code 104)
1	Chief of Naval Research (Code 418)
1	Chief of Naval Operations (Op-75)
1	Director, Naval Research Laboratory
2	CO-Dir., Naval Civil Engineering Laboratory (Huddleston, Document Library)
3	CO, Office of Naval Research, Branch Office, London
1	Supt., Naval Postgraduate School, Monterey
1	NRDL Laboratory Representative (Attmore)
	ARMY
1	Chief of Research and Development (Atomic Office)
1	CO, Nuclear Defense Laboratory (Rexroad, Schumchyk, Futterer)
1	Commander, Nuclear Defense Laboratory (Library)
3	Army Library TAGO, Civil Defense Unit
1	CO, Army Materials Research Agency (Weeks)
1	Assistant Secretary of the Army (R&D)
2	Shelter Research Division, OCD (Landdeck, Buchanan)
4	Army Ballistic Research Laboratory (Allen, Ethridge, Budka, Document Library)
1	USACDC Institute of Nuclear Studies
3	Office of Civil Defense (FitzSimmons, Stangler, Greene)
50	Office of Civil Defense (Ass't Director for Research)

AIR FORCE

1	Chief, Systems Engineering Group (SEPIR)
1	Director, USAF Project RAND
1	Director, Air University Library, Maxwell AFB
1	Air Force Institute of Technology (Nuclear Engineering Facility)

OTHER DOD ACTIVITIES

3	Dir., Defense Atomic Support Agency (Library, Daniel, Alfonte)
1	Commander, TC/DASA, Sandia Base (TCTG5, Library)
1	Office of Emergency Planning (R&D)
1	National Military Command System Support Center, BE 685
20	Defense Documentation Center

AEC ACTIVITIES AND OTHERS

1	Atomic Energy Commission, Washington
1	Atomics International (Ashley)
2	Battelle Memorial Institute
2	Conesco, Inc. (Batter, Velletri)
1	Division of Biology and Medicine, AEC (Deal)
1	Edgerton, Germeshausen and Grier (Burson)
2	IIT Research Institute (Sevin, Terrell)
1	Kansas State University (Kimel)
1	Los Alamos Scientific Laboratory (Document Library)
1	National Academy of Sciences (Park)
1	National Aeronautics and Space Administration (Reetz)
1	NASA, Lewis Research Center
3	National Bureau of Standards (Library, Eisenhauer, Berger)
1	New York University (Kalos)
1	North Carolina State University (Doggett)
5	Oak Ridge National Laboratory (Auxier, Zobel, Clifford, Penny, Library)
1	Oak Ridge National Laboratory (Radiation Shielding Information Center)
1	Opticals Materials, Inc. (Held)
1	Ottawa University (Spencer)
2	Pennsylvania State University (Foderaro, Kummer)
1	Purdue University. (Scott)
2	Radiation Research Associates (Wells, Schaeffer)
1	Research Triangle Institute (Parsons)
1	United Nuclear Corporation (Mittleman)
15	Division of Technical Information Extension, Oak Ridge

USNRDL

25 Technical Information Division

DISTRIBUTION DATE: 28 December 1966

UNCLASSIFIED
Security Classification

DOCUMENT CONTROL DATA - R&D

(Security classification of title, body of abstract and indexing annotation must be entered when the overall report is classified)

1. ORIGINATING ACTIVITY (Corporate author) U.S. Naval Radiological Defense Laboratory San Francisco, California 94135	2a. REPORT SECURITY CLASSIFICATION UNCLASSIFIED 2b. GROUP

3. REPORT TITLE

EXPERIMENTAL AND CALCULATED ESTIMATES OF THE SHIELDING EFFECTIVENESS OF COMPARTMENTED STRUCTURES EXPOSED TO FALLOUT

4. DESCRIPTIVE NOTES (Type of report and inclusive dates)

5. AUTHOR(S) (Last name, first name, initial)

Shumway, Bruce,W.

6. REPORT DATE 28 December 1966	7a. TOTAL NO. OF PAGES 58	7b. NO. OF REFS 12
8a. CONTRACT OR GRANT NO. b. PROJECT NO. c. OCD-PS-64-92, Work Unit 1111B d.	9a. ORIGINATOR'S REPORT NUMBER(S) USNRDL-TR-1045 9b. OTHER REPORT NO(S) (Any other numbers that may be assigned this report)	

10. AVAILABILITY/LIMITATION NOTICES

Distribution of this document is unlimited.

11. SUPPLEMENTARY NOTES	12. SPONSORING MILITARY ACTIVITY Office of Civil Defense Washington, D.C. 20310

13. ABSTRACT

Exposure reduction factors were measured inside six compartmented steel structures having different wall thicknesses ranging from 1/4 to 1-1/2 in. These were exposed to radiation from fallout of varying age from three to nine days. Calculations based upon the Nelms-Cooper gamma-ray spectrum at H + 1.12 hours were made for selected compartments in each of the structures following procedures given in the Office of Civil Defense Professional Manual, PM-100-1. Comparison of experiment and calculation reveals a sensitivity to spectral changes and shows that protection is greater during the periods D + 3 to D + 9 days than at H + 1.12 hours. Overall agreement is generally satisfactory. The calculational methods for radiation through floors, however, appear to be inadequate.

Spectra measured on site at D + 3 and D + 9 days are given.

DD FORM 1 JAN 64 1473

UNCLASSIFIED
Security Classification

UNCLASSIFIED
Security Classification

14. KEY WORDS	LINK A ROLE	LINK A WT	LINK B ROLE	LINK B WT	LINK C ROLE	LINK C WT
Protection γ Rays Fallout Compartmentation Civil Defense						

INSTRUCTIONS

1. ORIGINATING ACTIVITY: Enter the name and address of the contractor, subcontractor, grantee, Department of Defense activity or other organization *(corporate author)* issuing the report.

2a. REPORT SECURITY CLASSIFICATION: Enter the overall security classification of the report. Indicate whether "Restricted Data" is included. Marking is to be in accordance with appropriate security regulations.

2b. GROUP: Automatic downgrading is specified in DoD Directive 5200.10 and Armed Forces Industrial Manual. Enter the group number. Also, when applicable, show that optional markings have been used for Group 3 and Group 4 as authorized.

3. REPORT TITLE: Enter the complete report title in all capital letters. Titles in all cases should be unclassified. If a meaningful title cannot be selected without classification, show title classification in all capitals in parenthesis immediately following the title.

4. DESCRIPTIVE NOTES: If appropriate, enter the type of report, e.g., interim, progress, summary, annual, or final. Give the inclusive dates when a specific reporting period is covered.

5. AUTHOR(S): Enter the name(s) of author(s) as shown on or in the report. Enter last name, first name, middle initial. If military, show rank and branch of service. The name of the principal author is an absolute minimum requirement.

6. REPORT DATE: Enter the date of the report as day, month, year; or month, year. If more than one date appears on the report, use date of publication.

7a. TOTAL NUMBER OF PAGES: The total page count should follow normal pagination procedures, i.e., enter the number of pages containing information.

7b. NUMBER OF REFERENCES: Enter the total number of references cited in the report.

8a. CONTRACT OR GRANT NUMBER: If appropriate, enter the applicable number of the contract or grant under which the report was written.

8b, 8c, & 8d. PROJECT NUMBER: Enter the appropriate military department identification, such as project number, subproject number, system numbers, task number, etc.

9a. ORIGINATOR'S REPORT NUMBER(S): Enter the official report number by which the document will be identified and controlled by the originating activity. This number must be unique to this report.

9b. OTHER REPORT NUMBER(S): If the report has been assigned any other report numbers *(either by the originator or by the sponsor)*, also enter this number(s).

10. AVAILABILITY/LIMITATION NOTICES: Enter any limitations on further dissemination of the report, other than those imposed by security classification, using standard statements such as:

(1) "Qualified requesters may obtain copies of this report from DDC."

(2) "Foreign announcement and dissemination of this report by DDC is not authorized."

(3) "U. S. Government agencies may obtain copies of this report directly from DDC. Other qualified DDC users shall request through
________________."

(4) "U. S. military agencies may obtain copies of this report directly from DDC. Other qualified users shall request through
________________."

(5) "All distribution of this report is controlled. Qualified DDC users shall request through
________________."

If the report has been furnished to the Office of Technical Services, Department of Commerce, for sale to the public, indicate this fact and enter the price, if known.

11. SUPPLEMENTARY NOTES: Use for additional explanatory notes.

12. SPONSORING MILITARY ACTIVITY: Enter the name of the departmental project office or laboratory sponsoring *(paying for)* the research and development. Include address.

13. ABSTRACT: Enter an abstract giving a brief and factual summary of the document indicative of the report, even though it may also appear elsewhere in the body of the technical report. If additional space is required, a continuation sheet shall be attached.

It is highly desirable that the abstract of classified reports be unclassified. Each paragraph of the abstract shall end with an indication of the military security classification of the information in the paragraph, represented as *(TS)*, *(S)*, *(C)*, or *(U)*.

There is no limitation on the length of the abstract. However, the suggested length is from 150 to 225 words.

14. KEY WORDS: Key words are technically meaningful terms or short phrases that characterize a report and may be used as index entries for cataloging the report. Key words must be selected so that no security classification is required. Identifiers, such as equipment model designation, trade name, military project code name, geographic location, may be used as key words but will be followed by an indication of technical context. The assignment of links, roles, and weights is optional.

DD FORM 1 JAN 64 1473 (BACK)

UNCLASSIFIED
Security Classification